What Interbank Rates Tell Us About Time-Varying Disaster Risk*

Hitesh Doshi Hyung Joo Kim Sang Byung Seo

C.T. Bauer College of Business, University of Houston

November 12, 2019

Abstract

We estimate time-varying disaster risk using interbank rates and their options. The identification of disaster risk has remained a significant challenge due to the rarity of macroeconomic disasters. We make an identification assumption that macroeconomic disasters coincide with banking disasters – extremely unlikely events in which the interbank market fails and investors suffer significant losses. Based on our flexible reduced-form setup, interbank rates together with their options allow us to extract the short-run and long-run components of disaster risk. Our estimation results serve as an external validity test of rare disaster models, which are typically calibrated to match stock moments.

*Doshi: hdoshi@bauer.uh.edu; Kim: hjkim@bauer.uh.edu; Seo: sseo@bauer.uh.edu. We thank Hui Chen, Kris Jacobs, Mete Kilic, Praveen Kumar, Jessica Wachter, Nancy Xu, and seminar participants at the University of Houston and the 2019 FMA annual meeting for helpful comments.

1 Introduction

As an explanation for puzzles in macro-finance, the rare disaster literature has received ample attention (for a comprehensive review, see Tsai and Wachter, 2015). The fundamental notion behind rare disasters is to put more weight on events that are extremely bad, albeit unlikely. Rietz (1988) and Barro (2006) introduce and formalize the rare disaster mechanism to explain the equity premium puzzle. More recently, Gabaix (2012), Gourio (2012), and Wachter (2013) incorporate the time variation in the probability or severity of disasters to account for puzzles related to volatility and return predictability.

However, rare disaster models have also received their fair share of criticism. For example, rare disasters are often referred to as "dark matter" because of the rarity of their observations and the obscurity of their source.[1] These criticisms point to the fact that it is difficult to reliably estimate the parameters associated with disasters. In line with this, Chen, Dou, and Kogan (2019) raise concerns with regard to overfitting in-sample data: if a disaster model excessively overfits in-sample data, then the model implication would be sensitive to small perturbations of disaster parameters. Estimating time-varying disaster risk is even more challenging. Cochrane (2017) considers time-varying probabilities of disasters as "dark energy" unless there is a way to independently anchor them to an external data source.

In this paper, we address these issues by estimating the time variation in disaster risk using interbank rates and their options. First, we define *banking disasters* as extremely unlikely events in which the interbank market among major banks collapses, resulting in substantial losses for market participants. Then, we capture the risk of consumption disasters by that of banking disasters, assuming that the two types of events coincide. The connection between the two has been empirically supported; for example, Reinhart and Rogoff (2013)

[1] In order to describe an extreme and rare economic downturn, the literature defines macroeconomic disasters as an severe drop in real consumption per capita (e.g. Barro, 2006; Barro and Ursúa, 2008; Gabaix, 2012; Wachter, 2013) or as a significant reduction in total factor productivity (e.g. Gourio, 2012).

point out that virtually all consumption disasters documented by Barro and Ursúa (2008) were accompanied by severe systemic banking crises.[2]

Intuitively, this assumption provides a direct link between disaster risk and the interbank market. Hence, based on interbank rates and their options, it is possible to estimate the dynamics of time-varying disaster risk, with the aid of a model. Specifically, we adopt a flexible reduced-form setup where the nominal pricing kernel is comprised of Brownian and Poisson shocks to the four state variables of the economy: (1) real consumption growth, (2) expected inflation, (3) short-run disaster risk, and (4) long-run disaster risk. Under our affine framework where the instantaneous nominal risk-free rate is modeled as a linear function of the state variables, we derive the model expressions for the interbank rate and the Treasury rate for each maturity. We, then, show that their gap (the so-called TED spread) is highly informative about disaster risk, as it only depends on the two disaster-related state variables.

In addition to the TED spread, we take advantage of interest rate caps and swaptions, which are essentially option contracts on future interbank rates. A cap consists of a series of caplets, each of which can be viewed as a call option on the LIBOR. A swaption provides its holder the right to enter into an interest rate swap that exchanges floating coupons based on the LIBOR with fixed coupons based on the strike interest rate. With slight approximations, we express the prices of caps and swaptions in closed form up to ordinary differential equations using the transform method of Duffie, Pan, and Singleton (2000).

We estimate the model parameters via maximum likelihood estimation using the data from January 1997 to December 2017. As a result, we obtain parameter estimates whose signs and magnitudes are economically sensible. The model-implied time series for interest rates,

[2]The general idea of linking macroeconomic crises and banking crises has been well established in the literature. Bernanke (1983) argues that the failure of a substantial fraction of U.S. banks was the primary reason behind the Great Depression. Moreover, Allen, Bali, and Tang (2012) and Giesecke, Longstaff, Schaefer, and Strebulaev (2014) empirically compare the risk of financial sector defaults with that of non-financial corporate defaults and find that the former influences macroeconomic downturns, whereas the latter does not.

caps, and swaptions mimic their data counterparts reasonably well. Note that our utmost focus is on the model parameters that are associated with disaster risk: the unconditional disaster intensity is estimated to be 2.39%, implying 2.39 disasters per century on average. Overall, our results provide additional guidelines that can help discipline the calibration of rare disaster models.

An important advantage of our estimation is that it is possible to extract the short-run and long-run components of latent disaster risk through a filtering approach. Specifically, we adopt the extended Kalman filter because caps and swaption prices are nonlinear functions of the latent and observable state variables. From a sensitivity analysis, we discover that the short-run component of disaster risk is mainly identified by the TED spread with a short maturity. In contrast, the long-run component of disaster risk is primarily filtered out through caps and swaptions whose payoffs are contingent on future interbank rates over a long horizon. Importantly, the forward-looking information from interest rate options plays a crucial role in estimating not only the level but also the whole dynamics of disaster risk.

This paper's results emphasize that the interbank market can potentially be useful for overcoming the criticisms of rare disaster models, which are typically calibrated to match stock data. Our estimation is independent of equity market moments and, thus, serves as an external validity test of the models. The parameter estimates suggest that disaster risk is significant in magnitude and in variation, strongly supporting macro-finance models with the rare disaster mechanism. In addition, based on the filtered time series of the short-run and long-run components of disaster risk, we verify the testable implications that disaster risk should be associated with various conditional moments and returns in the equity market. All in all, our findings corroborate the disaster-based explanation of various asset pricing puzzles.

We contribute to the rare disaster literature by estimating the time-varying risk of eco-

nomic disasters. Granted, we are not the first to attempt to quantify the time series variation in disaster risk. For example, Berkman, Jacobsen, and Lee (2011) proxy the perceived disaster probability by a crisis severity index, constructed based on the number of international political crises. Manela and Moreira (2017) create a text-based disaster concern measure, called news implied volatility (NVIX), using the words in front-page articles of the Wall Street Journal. Rather than proposing another index that potentially correlates with disaster risk, our goal is to directly estimate the risk of consumption disasters under the identification assumption that consumption disasters coincide with banking disasters. A key advantage of our framework is that it is possible to exploit the information contained in interbank rates and their options, which allows us to separately extract the short-run and long-run components of disaster risk.

Our estimation relies on the pricing data on interest caps and swaptions. Prior studies, including Longstaff, Santa-Clara, and Schwartz (2001), Han (2007), and Trolle and Schwartz (2009), mainly concentrate on the relative pricing of caps and swaptions. However, the literature has paid little attention to what these financial instruments imply about the aggregate economy or other financial markets. We explore the economic content of caps and swaptions by focusing on the fact that their payoffs are contingent on future interbank rates. We confirm that interbank rate options indeed contain valuable information about the risk of banking disasters.

Our paper relates to the literature on understanding the source of interbank risk. Michaud and Upper (2008), Taylor and Williams (2009), Filipović and Trolle (2013), and McAndrews, Sarkar, and Wang (2017) decompose interbank risk into a pure credit component and a liquidity component to examine how they distinctively affect interbank risk. In contrast, we do not make such a distinction. We study the possibility of extreme tail events implied by the total risk of the interbank market, regardless of whether it originates from bank-specific

default risk or systemic liquidity risk.

The findings of this paper also potentially relate to the growing literature on the role of financial intermediaries in asset pricing. He and Krishnamurthy (2013) and Brunnermeier and Sannikov (2014) argue that intermediaries, rather than households, act as marginal investors and, therefore, their financial constraints are key drivers of market risk premia. Adrian, Etula, and Muir (2014) and He, Kelly, and Manela (2017) empirically support the theory by showing that intermediary-induced factors outperform traditional risk factors in explaining asset returns in various markets. Although our analysis mainly concerns economic disasters, the reduced-form pricing kernel we adopt has properties that are isomorphic to those of an intermediary-based pricing kernel: when the interbank market is hit by a shock (which is modeled as a shock to the risk of banking disasters in our framework), the pricing kernel responds and generates risk premia. Our results hint that the disaster-based explanation and the intermediary-based explanation of asset markets might share common microfoundations.

The rest of this paper proceeds as follows. Section 2 describes the model and Section 3 describes the data. Section 4 explains how we estimate the model and extract time-varying disaster risk. Section 5 reports the estimation results and discusses their implications. Section 6 concludes.

2 Model

2.1 The Risk of Banking Disasters and the TED Spread

We define banking disasters as extremely unlikely events in which the interbank market fails and market participants suffer significant losses. In this paper, we do not model the behaviors of banks nor the structure of the interbank market, which can potentially generate

banking disasters in an endogenous fashion. Instead, we simply specify the occurrence of banking disasters using a Poisson process N_t, as our focus is on empirically characterizing time-varying disaster risk. Following Seo and Wachter (2018), we assume that the Poisson process has stochastic intensity λ_t whose dynamics are described by

$$\begin{aligned} d\lambda_t &= \kappa_\lambda(\xi_t - \lambda_t)dt + \sigma_\lambda\sqrt{\lambda_t}dB_{\lambda,t}, \\ d\xi_t &= \kappa_\xi(\bar{\xi} - \xi_t)dt + \sigma_\xi\sqrt{\xi_t}dB_{\xi,t}, \end{aligned}$$

where ξ_t is the time-varying mean of instantaneous disaster risk λ_t. Simply put, λ_t and ξ_t represent the short-run and long-run components of disaster risk, respectively.

Let L_t denote the time-t face value of interbank lending. In the event of a banking disaster, this face value, or the expected principal payment, significantly reduces, whereas it remains constant otherwise. By defining $Z_{L,t} < 0$ as a random variable that captures the size of banking disasters, it follows that

$$L_t = \begin{cases} e^{Z_{L,t}}L_{t^-} & \text{if a banking disaster occurs at time } t, \\ L_{t^-} & \text{otherwise,} \end{cases}$$

or, equivalently,

$$\frac{dL_t}{L_{t^-}} = \left(e^{Z_{L,t}} - 1\right) dN_t.$$

Under this simple setup, it is intuitive that the TED spread, the difference between the 3-month interbank rate and the 3-month Treasury rate, contains important information about disaster risk. To illustrate, we compare the expressions for interbank rates and Treasury rates. The pricing relation implies that the τ-maturity zero-coupon interbank rate can be derived as:

$$y_{i,t}^{(\tau)} = -\frac{1}{\tau}\log\mathbb{E}_t\left[\frac{M_{t+\tau}}{M_t}\cdot\frac{L_{t+\tau}}{L_t}\right], \tag{1}$$

where $\left[\frac{M_{t+\tau}}{M_t}\right]$ represents the nominal pricing kernel whose existence is guaranteed under no arbitrage. While interbank lending contracts are potentially subject to partial defaults, nominal government bonds always pay back the promised amount at the end of their maturity. The τ-maturity zero-coupon government bond yield (or simply, Treasury rate) is calculated as:

$$y_{g,t}^{(\tau)} = -\frac{1}{\tau} \log \mathbb{E}_t \left[\frac{M_{t+\tau}}{M_t} \cdot 1 \right]. \tag{2}$$

Comparing equations (1) and (2) suggests that changes in disaster risk have a direct effect on the TED spread, defined as $\left[y_{i,t}^{(0.25)} - y_{g,t}^{(0.25)}\right]$. When disaster risk rises, the expectation of the future payoff $\left[\frac{L_{t+\tau}}{L_t}\right]$ decreases, which pushes interbank rates upward. However, this effect is missing for Treasury rates as the future payoff from default-free government bonds is always 1. As a result, the TED spread widens when disaster risk increases.

These equations also suggest that fluctuations in disaster risk or in other potential risk factors can have indirect effects on interbank rates and Treasury rates through the pricing kernel. However, if risk factors only impact the pricing kernel but not the future payoff $\left[\frac{L_{t+\tau}}{L_t}\right]$, they will move interbank rates with the same degree as Treasury rates, leaving the TED spread unchanged. Since the distribution $\left[\frac{L_{t+\tau}}{L_t}\right]$ only depends on λ_t and ξ_t, this suggests that risk factors that are orthogonal to λ_t and ξ_t will have no impact on the TED spread. Below, we show in our fairly flexible setup that the TED spread only depends on instantaneous disaster risk λ_t and its time-varying mean ξ_t, confirming this intuition.

2.2 Interbank Rates and Treasury Rates

Equations (1) and (2) make it clear that we need a nominal pricing kernel $\left[\frac{M_{t+\tau}}{M_t}\right]$ to derive the specific expressions for zero-coupon yields on interbank lending and on government bonds. Our pricing kernel is reduced-form in the sense that we exogenously specify its dynamics. Whereas the pricing kernel in an equilibrium model is typically pinned down by the interplay

between investors' preferences and endowment processes, the pricing kernel in our setup is written in a general form so that it can be directly estimated using data.

Before we specify the pricing kernel, we establish the state variables in the economy. In addition to the two factors that concern variable disaster risk (λ_t and ξ_t), we take two more variables that are typically used to capture the state of the economy: real consumption and expected inflation. First of all, we assume that real consumption follows an affine jump diffusion process,

$$\frac{dc_t}{c_{t^-}} = \mu_c dt + \sigma_c dB_{c,t} + \left(e^{Z_{c,t}} - 1\right) dN_t, \tag{3}$$

where $B_{c,t}$ is a standard Brownian motion. Equation (3) implies that when a banking disaster occurs ($dN_t = 1$), log consumption drops by $Z_{c,t}$. It is worth mentioning that we are agnostic about how banking disasters lead to macroeconomic disasters or vice versa. For our empirical analyses, it suffices that these two types of extreme events are associated with each other, as evidenced by Reinhart and Rogoff (2013). Consistent with the rare disaster literature, we assume that $Z_{c,t} = Z_{L,t} < 0$ follows the empirical distribution of Barro and Ursúa (2008). We plot this distribution in Panel A of Figure 1.

We also choose expected inflation as a relevant state variable following the interest rate term structure literature. We assume that the expected inflation process q_t solves the stochastic differential equation:

$$dq_t = \kappa_q(\bar{q} - q_t)dt + \sigma_q dB_{q,t} + Z_{q,t}dN_t, \tag{4}$$

where $B_{q,t}$ is a standard Brownian motion. As highlighted in Tsai (2015), it is necessary for macroeconomic disasters to coincide with positive jumps in expected inflation in order to generate an upward-sloping term structure of nominal interest rates. For parsimony, we

capture this commonality by assuming that q_t is also subject to the same Poisson process N_t and that the jump size random variable $Z_{q,t}$ is, on average, positive. Specifically, we construct the empirical distribution of $Z_{q,t}$ by compiling inflation rates during consumption disasters.[3] We present this distribution in Panel B of Figure 1.

We assume that Brownian shocks ($dB_{c,t}$, $dB_{\lambda,t}$, $dB_{\xi,t}$, $dB_{q,t}$) are independent of one another and of a Poisson shock (dN_t). These five independent shocks to the four state variables constitute the shocks to the nominal pricing kernel:

$$\frac{dM_t}{M_{t^-}} = -r_t dt + \theta_c dB_{c,t} + \theta_\lambda \sqrt{\lambda_t} dB_{\lambda,t} + \theta_\xi \sqrt{\xi_t} dB_{\xi,t} + \theta_q dB_{q,t} + \left[\left(e^{\theta_N Z_{c,t}} - 1 \right) dN_t - \lambda_t \mathbb{E}\left[e^{\theta_N Z_{c,t}} - 1 \right] dt \right], \quad (5)$$

where r_t represents the instantaneous nominal risk-free rate. To preserve the affine structure of our setup, we represent r_t as a linear function of the state variables, similar to Ang and Piazzesi (2003), and Joslin, Le, and Singleton (2013):

$$r_t = \delta_0 + \delta_\lambda \lambda_t + \delta_\xi \xi_t + \delta_q q_t. \quad (6)$$

Note that the pricing kernel fully characterizes the risk-neutral measure, as the Radon-Nikodym derivative process of the risk-neutral measure with respect to the physical measure equals $\left[M_t \int_0^t r_s ds \right]$. In Appendix A.1, we derive the risk-neutral dynamics of the underlying processes using Girsanov's theorem.

Based on the pricing kernel specified above, we finally calculate the expressions for $y_{i,t}^{(\tau)}$ and $y_{g,t}^{(\tau)}$ in equations (1) and (2). We show that both interbank rates and Treasury rates are

[3]The Barro-Ursua dataset contains a few extreme hyperinflation events, such as the hyperinflation of Weimar Germany in the 1920s where the inflation rate exceeded 3,000%. Given that the number of historical consumption disasters is only 89, such extreme outliers completely dominate the moment generating function of $Z_{q,t}$. Thus, we exclude the observations that fall more than 3 times the interquartile range above the third quartile. No observations fall more than 3 times the interquartile range below the first quartile.

linear in state variables λ_t, ξ_t, and q_t:

$$y_{i,t}^{(\tau)} = -\frac{1}{\tau}\left[a_i(\tau) + b_{i,\lambda}(\tau)\lambda_t + b_{i,\xi}(\tau)\xi_t + b_q(\tau)q_t\right], \tag{7}$$

$$y_{g,t}^{(\tau)} = -\frac{1}{\tau}\left[a_g(\tau) + b_{g,\lambda}(\tau)\lambda_t + b_{g,\xi}(\tau)\xi_t + b_q(\tau)q_t\right], \tag{8}$$

where deterministic functions a_i, a_g, $b_{i,\lambda}$, $b_{g,\lambda}$, $b_{i,\xi}$, $b_{g,\xi}$, and b_q solve the ordinary differential equations derived in Appendix A.2.

One notable aspect when comparing equations (7) and (8) is that the loading on expected inflation q_t is identical for both types of interest rates. Therefore, for each maturity τ, the difference between the interbank rate and the Treasury rate becomes a function of disaster risk (λ_t and ξ_t) alone, confirming the intuition from Section 2.1 that the TED spread is only sensitive to disaster risk. Although the TED spread typically refers to the gap in the 3-month yields, we expand its definition for an arbitrary τ and refer to it as the τ-maturity TED spread hereafter:

$$\text{TED}_t^{(\tau)} = -\frac{1}{\tau}\Big[\big(a_i(\tau) - a_g(\tau)\big) + \big(b_{i,\lambda}(\tau) - b_{g,\lambda}(\tau)\big)\lambda_t + \big(b_{i,\xi}(\tau) - b_{g,\xi}(\tau)\big)\xi_t\Big]. \tag{9}$$

2.3 Options on Interbank Rates

In this section, we introduce derivative contracts called caps and swaptions whose payoffs depend on future interbank rates. When discussing their payoffs and pricing, it is convenient to introduce the following notation:

$$P_i(t, t+\tau) = \exp\left(-\tau \cdot y_{i,t}^{(\tau)}\right). \tag{10}$$

In other words, $P_i(t, t+\tau)$ represents the time-t value of \$1 zero-coupon interbank lending maturing at time $t+\tau$.

In addition, we need the expression for the 6-month LIBOR in the model. Recall that the 6-month LIBOR is a simple interest rate and, therefore, is not exactly the same as the continuously compounded rate $y_{i,t}^{(0.5)}$. In fact, the 6-month LIBOR rate is expressed as:

$$\text{LIBOR}_t = 2\left[\exp\left(\tau \cdot y_{i,t}^{(\tau)}\right) - 1\right] = 2\left(\frac{1}{P_i(t, t+0.5)} - 1\right). \tag{11}$$

An interest rate cap consists of a series of caplets that mature every 6 months.[4] Specifically, the first caplet matures 6 months from today, and the last caplet matures 6 months prior to the cap maturity date. Let T denote the time to maturity of a cap from today (time t), and K_c denote its strike interest rate. For notational convenience, we define $\Delta = 0.5$ and $t_j = t + \Delta j$.

The j-th caplet provides the holder of the cap with the right, not the obligation, to borrow a dollar at the rate of K_c between times t_j and t_{j+1}. If the future 6-month LIBOR at time t_j is higher than the strike K_c, this caplet is exercised and the holder borrows a dollar at the lower-than-the-fair interest rate. That is, the payoff from exercising the caplet is $\Delta \times \left(\text{LIBOR}_{t_j} - K_c\right)$. This payoff occurs at time t_{j+1} because the interest payment is made at the end of the borrowing period.

Since the cap is a collection of a $m_T = \left(\frac{T}{\Delta} - 1\right)$ number of caplets, the time-t cap value is calculated as:

$$V_{\text{cap}}^{(T)}(t, K_c) = \sum_{j=1}^{m_T} \mathbb{E}_t^Q \left[\exp\left(-\int_t^{t_{j+1}} r_s ds\right)\left[\Delta \times \left(\text{LIBOR}_{t_j} - K_c\right)\right]^+\right], \tag{12}$$

where Q represents the risk-neutral measure (see Appendix A.1).[5] In Appendix A.3, we

[4]More precisely, a conventional cap contract traded in the market is a collection of caplets that mature every 3 months. As documented by Longstaff, Santa-Clara, and Schwartz (2001), assuming semi-annually spaced caplets for computational convenience is innocuous, generating a negligible difference when it comes to Black-implied volatilities.

[5]We can obtain the same result if we multiply the cap payoff by the pricing kernel and take the expectation under the physical measure. Following the convention in the literature on interest rate derivatives, we use

demonstrate that equation (12) can be computed using the transform analysis of Duffie, Pan, and Singleton (2000).

An interest rate swaption grants the holder the right, not the obligation, to enter into an interest rate swap (IRS). There are two types of swaptions. When exercised, a payer swaption delivers an IRS where the holder pays the fixed leg and receives the floating leg (a payer IRS); a receiver swaption delivers an IRS where the holder receives the fixed leg and pays the floating leg (a receiver IRS). We now define T as the time to maturity of payer and receiver swaptions. Let K_s denote their strike interest rate. The tenor of the IRS at the maturity of the swaptions is denoted as $\bar{T}$. Under this notation, our swaptions of interest are often referred to as T-into-$\bar{T}$ swaptions.

The payer swaption is exercised if the future $\bar{T}$-maturity swap rate at time $t+T$ is larger than the strike K_s. In this case, the holder enters into a payer IRS contract and makes a profit by exchanging the fixed rate K_s (which is lower than the fair swap rate) for the floating rate. The profit, or the value of this payer IRS at time $t+T$, is simply the difference between its floating leg and its fixed leg. The floating leg is always 1 because it is equivalent to the value of a floating rate note whose coupons reset periodically. In contrast, the fixed leg is equivalent to the value of a dollar notional coupon bond with the (annualized) coupon rate of K_s:

$$V_{\text{fixed}}^{(\bar{T})}(t+T, K_s) = \Delta \left[K_s \sum_{j=1}^{\bar{T}/\Delta} P_i \left(t+T, t+T+j\Delta\right) \right] + P_i(t+T, t+T+\bar{T}). \tag{13}$$

Therefore, the time-t payer swaption value is expressed as:

$$V_{\text{pay}}^{(T,\bar{T})}(t, K_s) = \mathbb{E}_t^Q \left[\exp\left(- \int_t^{t+T} r_s ds \right) \left[1 - V_{\text{fixed}}^{(\bar{T})}(t+T, K_s) \right]^+ \right]. \tag{14}$$

the pricing relation under the risk-neutral measure.

Similarly, the receiver swaption is exercised if the future $\bar{T}$-maturity swap rate at time $t+T$ is smaller than the strike K_s. The time-t receiver swaption value is expressed as:

$$V_{\text{rcv}}^{(T,\bar{T})}(t, K_s) = \mathbb{E}_t^Q \left[\exp\left(-\int_t^{t+T} r_s ds \right) \left[V_{\text{fixed}}^{(\bar{T})}(t+T, K_s) - 1 \right]^+ \right]. \tag{15}$$

These equations suggest that interest rate swaptions can essentially be viewed as options on a coupon bond. Due to coupon payments, the expression for the coupon bond price contains multiple terms, which makes it impossible to calculate the expectations in equations (14) and (15) using the semi-analytic approach of Duffie, Pan, and Singleton (2000). To make the computation tractable, we adopt the so-called stochastic duration method implemented by Trolle and Schwartz (2009). This method enables us to accurately approximate the price of a coupon bond option by a constant multiplication of the price of a zero-coupon bond option (see, e.g., Wei, 1997; Munk, 1999). We provide a detailed description of the swaption pricing procedure in Appendix A.3.

3 Data

Our data sample consists of the following variables: Black-implied volatilities for caps and swaptions, interbank rates, Treasury rates, expected inflation, and real consumption per capita. All variables are sampled at a monthly frequency at the end of each month, from January 1997 to December 2017.

We download the pricing data on caps and swaptions from Bloomberg.[6] Caps and swaptions are typically quoted in terms of Black-implied volatilities. For each market price, the corresponding Black-implied volatility is found by backsolving the volatility term in the

[6]There are multiple sources for caps and swaptions data on Bloomberg. We mainly use the source "BBIR," which provides the Black-implied volatilities calculated based on LIBOR-swap curves. Since this data source provides the time series from April 2002, we complement it by adding the data from the source "CMPN" for the period between January 1997 and March 2002.

Black (1976) model.

Caps and swaptions in our sample are at-the-money forward (ATMF), meaning that the strike price of each option is equal to the current forward price of the underlying. Specifically, the strike price of a T-maturity ATMF cap is the T-maturity swap rate. The strike price of a T-into-$\bar{T}$ ATMF swaption is the forward swap rate between the option expiry (T years from today) and the underlying swap expiry ($T + \bar{T}$ years from today).

Interbank rates consist of 3-, 6-, and 12-month LIBOR rates as well as 2-, 3-, 5-, 7-, and 10-year swap rates, all of which are downloaded from Bloomberg. We also collect the Treasury rates with the same maturities from the Federal Reserve Bank of St. Louis. To make the data comparable with the model-implied interest rates, we need to convert the two types of interest rate term structures into continuously compounded zero curves. To do so, we adopt a procedure that is similar to Trolle and Schwartz (2009): we first transform raw interest rates into their corresponding par rates. Then, we use linear interpolation to construct par curves with maturities ranging from 6 months to 10 years with 6-month intervals. From these interpolated par curves, we extract smooth forward rate curves and, in turn, zero-coupon yield curves via the Nelson and Siegel (1987) parameterization.

The data on expected inflation is obtained from the Blue Chip Economic Indicators survey. This dataset provides the forecasts of inflation for the current calendar year and for the next calendar year. For each month, we calculate a proxy for the 1-year ahead expected inflation by calculating the weighted average between the two forecasts. Lastly, the monthly time series of real consumption per capita is from the Federal Reserve Bank of St. Louis.

4 Estimation Procedure

Estimating our model is computationally challenging. In each iteration of the MLE procedure, we need to evaluate the log-likelihood function. Due to cap/swaption pricing, this

requires numerically solving the system of complex-valued ordinary differential equations of Duffie, Pan, and Singleton (2000) several times. Furthermore, we have a large number of parameters to be estimated: 18 model parameters together with three additional parameters concerning measurement errors (described below). As a result, estimating all of these parameters at once in a single maximum likelihood estimation (MLE) is highly time-consuming.

To alleviate the computational burden, we first separately estimate the parameters μ_c, σ_c, κ_q, $\bar{q}$, and σ_q, which govern the normal-time dynamics of real consumption and expected inflation. This is possible because a consumption/banking disaster was absent during our sample period, implying that the observed time series of real consumption and expected inflation were completely driven by these five parameters. Specifically, μ_c and σ_c are estimated by maximizing the log-likelihood of the real consumption time series, conditional on no disasters. Similarly, κ_q, $\bar{q}$, and σ_q are estimated from the expected inflation time series via MLE.

We further reduce the dimension of our parameter space by putting a restriction on the value of δ_0. Taking expectations on both sides of equation (6) results in:

$$\mathbb{E}[r] = \delta_0 + \delta_\lambda \mathbb{E}[\lambda] + \delta_\xi \mathbb{E}[\xi] + \delta_q \mathbb{E}[q].$$

Here, we proxy the unconditional mean of the short rate ($\mathbb{E}[r]$) by the average 1-month risk-free rate ($\hat{\mathbb{E}}[r]$) from the CRSP dataset. Then, the value of δ_0 can be obtained as:

$$\delta_0 = \hat{\mathbb{E}}[r] - \delta_\lambda \bar{\xi} - \delta_\xi \bar{\xi} - \delta_q \hat{\mathbb{E}}[q],$$

where $\hat{\mathbb{E}}[q]$ is the average expected inflation during our sample period.

The remaining 15 parameters are now estimated within the main MLE procedure. We construct the likelihood function $\mathcal{L}$ under the assumption that we observe the following: (i)

3-, 6-, 12-month TED spreads, (ii) interbank rates and Treasury rates with 3-, 6-, 12-month, 2-, 3-, 5-, 7-, 10-year maturities, (iii) 2-, 3-, 4-, 5-, 7-, 10-year cap implied volatilities, and (iv) 1-into-4, 2-into-3, 3-into-2, 4-into-1, 3-into-7, 5-into-5 swaption implied volatilities. For notational simplicity, we let Y_t denote the vector of all these observations at time t.

To obtain the likelihood function $\mathcal{L}$, it suffices to derive the transition density of Y_t. Specifically, we define $\mathcal{L}_t$ as the likelihood of observing Y_t conditional on $Y_{t-\Delta t}$:

$$\mathcal{L}_t = \mathbb{P}\left(Y_t | Y_{t-\Delta t}\right),$$

where $\Delta t = 1/12$ represents monthly time intervals between observations. Not only does this transition density depend on the observable state variable q_t, but it also relies on the two latent variables λ_t and ξ_t.

In order to solve this filtering problem, we specify the state equation and the measurement equation in the state-space representation of our model. The state equation describes the dynamics of a latent state vector $S_t = [\lambda_t, \xi_t]^\top$. There are two ways to map the continuous-time dynamics of S_t into the discrete-time state equation. The first approach applies the Euler discretization to λ_t and ξ_t, and then finds the discrete-time relation between S_t and $S_{t-\Delta t}$. In contrast, the second approach finds the exact relation between S_t and $S_{t-\Delta t}$ without any approximation, and then discretizes the resulting relation. We adopt the latter approach following Chen and Scott (2003), as it better captures the square-root diffusions of the two latent processes. Consequently, we obtain the following linear state equation:

$$S_t = \eta + \Psi S_{t-\Delta t} + \epsilon_t, \quad \text{where } \mathbb{E}_{t-\Delta t}\left[\epsilon_t \epsilon_t^\top\right] = \Omega_{t-\Delta t}. \tag{16}$$

We provide the expressions for two-dimensional vector η, 2×2 matrix Ψ, and 2×2 time-varying covariance matrix Ω in Appendix B. Since ϵ_t is non-normal, we approximate it by

a normal distribution with the same covariance matrix. Prior studies document that this assumption is innocuous.[7]

Now, we turn to the measurement equation. We assume that Y_t is observed with a vector of measurement errors e_t:

$$Y_t = h(S_t, q_t) + e_t, \quad \text{where } \mathbb{E}_{t-\Delta t}\left[e_t e_t^\top\right] = Q. \tag{17}$$

Note that $h(\cdot)$ is a vector-valued function of the state variables that generate the model counterparts of the data. The mean-zero random vector e_t is normally distributed with covariance matrix Q. For parsimony, we assume that Q is determined by the following three parameters: the standard deviation of the measurement errors for TED spreads (σ_{SP}), the one for interest rates (σ_{ITR}), and the one for Black-implied volatilities (σ_{OPT}). All measurement errors are iid and are independent of one another.

The measurement equation clearly suggests that the linear Kalman filter cannot be used in our estimation. This is because h is not a linear function: cap/swaption prices as well as their Black-implied volatilities are nonlinear in the state variables. Therefore, we apply the extended Kalman filter, in which h is locally linearized at each set of predicted values of the state variables. In Appendix B, we provide a detailed description of how the extended Kalman filter is implemented under our setup.

In each iteration of the MLE procedure, we obtain not only the time series of the estimated latent variables $\left\{\hat{\lambda}_t,\ \hat{\xi}_t\right\}$, but also the time series of the transition densities $\{\mathcal{L}_t\}$ through this filtering process. Let $\{t_k\}_{k=1}^n$ denote monthly-spaced points in time when the data time series are observed. Then, the log-likelihood function for the entire observations can finally

[7] See, for example, Duan and Simonato (1999), Duffee (1999), Chen and Scott (2003), Trolle and Schwartz (2009), and Filipović and Trolle (2013).

be expressed as:

$$\log \mathcal{L} = \sum_{k=1}^{n} \log \mathcal{L}_{t_k}. \tag{18}$$

We obtain our parameter estimates by maximizing this log-likelihood function.[8]

5 Results

5.1 Parameter Estimates

Table 1 reports the values of our model parameters estimated through the MLE procedure, together with their robust standard errors in parentheses.[9] First of all, we can observe that the parameter values for consumption growth and expected inflation are economically sensible. During normal periods without disasters, consumption growth has a mean (μ_c) of 1.38% and a standard deviation (σ_c) of 0.81%, exactly consistent with the first two moments of the observed consumption time series in our sample. The parameter values for expected inflation are also in line with the corresponding data time series: the long-run mean ($\bar{q}$) is about 2%, the conditional volatility (σ_q) is 0.62%, and the monthly autocorrelation ($1-\kappa_q \Delta t$) is approximately 0.96.

Our main focus is on the model parameters that are associated with the dynamics of disaster risk. Table 1 shows that the unconditional disaster intensity (i.e. $E[\lambda] = E[\xi] = \bar{\xi}$) is estimated to be 2.39%, which indicates that investors expect, on average, 2.39 disasters per century. For comparison, note that Barro and Ursúa (2008) calibrate the frequency of economic disasters as 3.64% based on the long-term panel of international consumption time

[8]For robustness, we also run the penalized MLE by adopting the fragility measure of Chen, Dou, and Kogan (2019) as a penalty function. The fragility measure captures how much our estimated model overfits in-sample data relative to the baseline case, in which the model is estimated only based on interest rates without interbank options. While the penalized MLE slightly changes the point estimates of the model parameters, we find that the overall implications of the model remain intact.

[9]As described in Section 4, the parameter δ_0 is uniquely determined by other parameters and, hence, its standard error is not calculated.

series. There are two key differences between our approach and theirs. First, instead of relying on past consumption time series, we estimate the unconditional disaster likelihood from the pricing data on interbank rates and related options. Given the extremely infrequent nature of disasters, the frequency can be more robustly estimated by exploiting forward-looking information from asset prices. Second, unlike Barro and Ursúa (2008), our estimation is only based on U.S. data. Therefore, it is possible to interpret our parameter estimate as a U.S.-specific quantity. In fact, our estimate (i.e. 2.39%) is lower compared to what Barro and Ursúa (2008) report (i.e. 3.64%), presumably reflecting that the U.S. is relatively more stable than the global average.

In our model, disaster risk has a two-factor structure with λ_t and ξ_t. While both processes are estimated to be highly persistent with low mean reversion speed (κ_λ and κ_ξ), λ_t is relatively less persistent than ξ_t. This is intuitive because λ_t captures the short-run component of disaster risk, whereas ξ_t captures the long-run component. Consistent with this interpretation, λ_t exhibits a higher conditional volatility than ξ_t (i.e. $\sigma_\lambda > \sigma_\xi$). Overall, our results reveal that the estimated dynamics of disaster risk is fairly consistent with the calibration of Seo and Wachter (2018), who adopt the same two-factor disaster risk structure. In Section 5.3, we further characterize the time variation in disaster risk by examining the filtered time series of λ_t and ξ_t.

The estimated coefficients δ_λ, δ_ξ, and δ_q in Table 1 show how the three state variables λ_t, ξ_t, and q_t affect the nominal risk-free rate in our estimated model. We observe that the factor loadings on λ_t and ξ_t are negative. This is in accordance with the intuition behind the precautionary savings motive. When disaster risk rises, investors are inclined to save more to secure against future uncertainty, and this drives down the real risk-free rate in equilibrium. In contrast, the factor loading on expected inflation is positive. This can be explained by the so-called Fisher effect: the nominal risk-free rate is approximately the real risk-free rate

plus the expected inflation rate. Indeed, the magnitude of δ_q is close to 1, implying that an 1% increase in expected inflation leads to a roughly 1% increase in the nominal risk-free rate.

Additionally reported are the market prices of risk. We find that the signs of these four coefficients are reasonable. The market prices of diffusive risk (θ_λ, θ_ξ, and θ_q) are positive.[10] This suggests that the pricing kernel or investors' marginal utility rises when a positive Brownian shock ($dB_{\lambda,t}$, $dB_{\xi,t}$, or $dB_{q,t}$) is realized. In contrast, the market price of jump risk (θ_N) is negative. This indicates that $e^{\theta_N Z_{c,t}}$ is larger than 1, which subsequently implies that the pricing kernel goes up when a disaster occurs ($dN_t = 1$). All in all, we conclude that the signs and magnitudes of the model parameters from our estimation well comply with general economic intuition.

5.2 Implications for Interest Rates, Caps, and Swaptions

We now investigate whether our estimated model is capable of producing a reasonable fit to the market data on interest rates, caps, and swaptions. We first examine short-term interest rates by plotting the time series of the Treasury rate (Panel A), the interbank rate (Panel B), and the TED spread (Panel C) with a 3-month maturity in the data (solid blue line) and in the model (dashed red line). All interest rates are expressed as continuously compounded rates. As described in Section 2.2, the TED spread is also calculated as the difference between the interbank rate and the Treasury rate, both with continuous compounding.

Panel A of Figure 2 shows that at the beginning of our data sample from 1997 to 2001, the 3-month Treasury rate maintained a relatively stable level, fluctuating between 4% and 6%. Note that we can see a small dip toward the end of 1998, which corresponds to the Long-Term Capital Management (LTCM) crisis. Starting from 2001, the Treasury rate entered a steady

[10] In our estimation, θ_c is not identified because it is irrelevant for interest rates and interest rate options.

downward trend up until 2004. During this time, the Federal Reserve lowered the federal funds rate from 6% to 1%, as investors faced high economic and financial uncertainty due to the 2001 recession, the September 11 attacks, and the Afghanistan War. This period of expansionary monetary policy was followed by a 3-year period of contractionary monetary policy due to a housing market bubble and high inflation, causing the Treasury rate to gradually increase. From 2007, the Treasury rate began to rapidly decline again when the economy was hit by the subprime mortgage crisis, and eventually reached a level close to zero. Since then, the Treasury rate maintained a very low level until the Federal Reserve started raising interest rates in 2015.

The 3-month interbank rate in Panel B of Figure 2 also exhibits a similar time series pattern in general compared to the 3-month Treasury rate, although its magnitude is slightly larger. However, a distinctive pattern is observed around September 2008 when Lehman Brothers filed for bankruptcy. In contrast to the Treasury rate, the interbank rate sharply increased, reflecting a serious risk of a potential systemic meltdown in financial markets.

This event is more noticeable from the time series of the TED spread in Panel C of Figure 2. While the TED spread stayed at a high level between 2007 and 2009 during the Great Recession period, an exceptionally high value of over 3% was seen in September 2008. Also of note is the early part of the sample between 1997 and 2000. Not only was the TED spread relatively high, it significantly fluctuated with a cluster of small peaks due to the events surrounding the 1997 Asian financial crisis, the 1998 Russian moratorium, the LTCM crisis, and the dot-com bubble burst.

From these three panels of Figure 2, we find that our model is able to account for these patterns of the Treasury rates and interbank rates as well as their differences. The dashed red lines that represent the model-implied time series closely resemble the solid blue lines that represent the data time series, peaking and dipping around the same points in time.

This is the case for longer-maturity interest rates as well: in Figure 3, we find that the model-implied Treasury rates and interbank rates with 2-, 5-, and 10-year maturities mimic their data counterparts fairly well. Granted, the fit is not perfect. For instance, although our model matches the low-frequency trend of the 10-year Treasury rates and interbank rates relatively well, it does not capture some of their high-frequency short-run fluctuations, as can be seen in Panels C and F of Figure 3. Instead of adding more factors to improve the fit, we choose to keep our model simple and parsimonious, as our goal is to extract time-varying disaster risk, not to fit interest rates.

We now turn to caps and swaptions. Panels A, B, and C of Figure 4 present the time series of the Black-implied volatilities for the 2-, 5-, and 10-year caps, and Panels D, E, and F present those for the 2-into-3, 1-into-4, and 5-into-5 swaptions. In each panel, the solid blue line denotes the data, and the dashed red line denotes the model.

Before discussing the model outcomes, we point out that interpreting the magnitude and the time series variation of Black-implied volatilities in the data is not straightforward. For example, the Black-implied volatilities for the 2-year cap are generally much higher than those for the 5-year or 10-year cap. Why is this the case? Furthermore, in all of the panels in Figure 4, the Black-implied volatilities between 2010 and 2016 are exceptionally high even compared to the Great Recession period between 2007 and 2009.

Why do the time series and cross sectional patterns of Black-implied volatilities seem odd? The reason is that the Black formulas for caps and swaptions are derived under the assumption that a forward interest rate follows a log-normal distribution. That is, implied volatilities for caps and swaptions, converted from their market prices through the Black formulas, represent yield volatilities, not bond price volatilities. Hence, the level of Black-implied volatilities simply tends to be higher when the level of forward interest rates is lower. This explains why Black-implied volatilities in the data turn out to be so high in

the post Great Recession period, despite relatively lower uncertainty in the market: a 1% expected movement in a yield corresponds to 20% yield volatility if the yield is currently at 5%, whereas it corresponds to 100% if the yield is at 1%.

To illustrate the distinction between yield volatilities versus equivalent bond volatilities, Figure 5 juxtaposes the 1-month-into-10-year swaption-implied volatility (solid blue lines) with the TYVIX (dotted green lines), which measures the risk-neutral expectation of future 1-month volatility of 10-year Treasury note futures. In Panel A, we can see that these two quantities look completely different in terms of their levels and their patterns. This is because the swaption implied volatility is a yield volatility, whereas the TYVIX is a bond price volatility; in a sense, Panel A compares apples to oranges.

In order to compare apples to apples, we convert the Black-implied volatility into the equivalent price volatility of a 10-year zero-coupon bond starting a month from today. This is simply done using the following relation between yield volatility and its equivalent bond volatility under the lognormality of the Black model:

$$\sigma_{\text{price}} = \tau \times y \times \sigma_{\text{yield}},$$

where, with a slight abuse of notation, τ is the maturity of the bond, and y is the given yield. In other words, by setting τ to be 10 years and y to be the forward interest rate between 1 month and 1 month plus 10 years, we obtain the forward-starting bond price volatility that corresponds to the 1-month-into-10-year swaption. In Panel B of Figure 5, we discover that the resulting time series of the equivalent bond price volatility is finally comparable to that of the TYVIX. Not only are their levels very similar, but their time series patterns closely resemble each other. Note that the swaption-equivalent bond price volatility is slightly higher than the TYVIX every single point in time. This is straightforward because the former is additionally affected by the systemic risk in the interbank lending market (i.e.

banking disasters). Consistently, the gap in their levels substantially widens during the Great Recession.

In sum, we conclude that it is more intuitive to compare the data and the model in terms of bond price volatilities rather than Black-implied volatilities. Figure 6 converts the Black-implied volatilities in the data and in the model into their equivalent forward-starting bond price volatilities. The Black-implied volatility for the T-maturity cap is converted into the price volatility of a bond that corresponds to its last caplet: a 6-month zero-coupon bond starting after $(T - 0.5)$ years and maturing after T years from today. As described above, the Black-implied volatility for the T-into-$\bar{T}$ swaption is converted to the price volatility of a $\bar{T}$-maturity zero-coupon bond starting T years from today.

Figure 6 shows that our model's fit to the data is not perfect. While the fit to short-maturity caps and short-tenor swaptions (Panels A, B, D, and E) is reasonably good, the model greatly exaggerates the fluctuations of longer-maturity caps and longer-tenor swaptions compared to the data (Panels C and F). It is not surprising that our model is not able to well match every cap or swaption. Prior studies document that it is challenging to jointly account for the pricing of caps and swaptions in crisis periods, even with a flexible statistical model featuring several latent processes (Longstaff, Santa-Clara, and Schwartz, 2001; Han, 2007; Trolle and Schwartz, 2009). We want to reiterate that our objective is not to fit the data perfectly. Rather, we attempt to characterize time-varying disaster risk by exploiting the information contained in caps and swaptions, whose payoffs depend on future interbank rates. For our purposes, we believe that our simple economic model does a reasonably good job in capturing the data overall.

5.3 Characterizing Time-Varying Disaster Risk

Our estimation procedure enables us to characterize the time variation in disaster risk via the extended Kalman filter. Figure 7 displays the filtered time series of the short-run disaster risk component λ_t (solid blue line) and the long-run disaster risk component ξ_t (dashed red line).

From the figure, it is clear that the instantaneous disaster risk λ_t is much more volatile than its time-varying mean ξ_t. Since λ_t is highly persistent, it sometimes significantly deviates from its mean value of 2.39% for extended periods of time. At the beginning of our sample, we can observe a few spikes around the LTCM crisis and the dot-com bubble burst, at which λ_t rose beyond 3%. While the instantaneous disaster risk hovered around a low level of 1% between 2002 and 2006, it abruptly increased to an extremely high level at the onset of the subprime mortgage crisis in 2007. During the subsequent 2-year period of severe economic downturns and financial market turmoil, λ_t jumped to a level above 5%. Specifically, when Lehman Brothers declared bankruptcy in September 2008, λ_t reached its highest value, exceeding 10%. After the crisis, the level of λ_t came back to a normal level, but we still can see some small peaks that are associated with economic and financial uncertainty, like in the European sovereign debt crisis.

While λ_t captures a fast-moving component of disaster risk, ξ_t captures a slow-moving component. The filtered time series in Figure 7 reveal that ξ_t is much less volatile than λ_t and moves slowly without deviating too much from its mean value. Moreover, we observe that ξ_t is far more persistent than λ_t: once it is hit by a large positive shock, it takes a long time for it to mean-revert back to its previous level. For instance, the level of ξ_t was still high during the post Great Recession period. This is in sharp contrast with the behavior of λ_t, whose level quickly dropped even before the crisis was over.

Which aspect of the data makes it possible for us to characterize the time variation in

λ_t and ξ_t, as discussed above? To understand how time-varying disaster risk is identified through our model, we conduct a sensitivity analysis. Figure 8 shows how TED spreads (Panel A) and Black-implied volatilities for caps (Panel B) and swaptions (Panel C) change when we vary λ_t or ξ_t from the 10th percentile to the 90th percentile of its filtered values. In each panel, the solid blue lines describe the sensitivity with respect to λ_t while fixing ξ_t at the median, whereas the dashed red lines describe the sensitivity with respect to ξ_t while fixing λ_t at the median. Expected inflation q_t is set at its median value in both cases. Lastly, the black dot in the middle of each bar graph represents a model value when λ_t and ξ_t are both at their median values.

Panel A of Figure 8 reveals that the short-run component of disaster risk λ_t is mainly identified by TED spreads. While TED spreads increase with both λ_t and ξ, they are much more sensitive to λ_t. For example, the 3-month TED spread moves substantially, ranging from 0.2% to 0.8%, when λ_t varies between the 10% and 90% percentiles. In contrast, the 3-month TED spreads barely change with respect to ξ_t, as can be seen in the panel.

These results are intuitive. The 3-month interbank rate is higher than the 3-month Treasury yield because it is further influenced by the risk of a banking disaster happening over a 3-month horizon. Therefore, their gap, the 3-month TED spread, is mostly sensitive to the short-run component of disaster risk. For the same reason, ξ_t plays a more noticeable role if a longer horizon is considered: from the panel, we find that the longest TED spread with a 12-month maturity is more responsive to changes in ξ_t, compared to the 3-month TED spread. However, the magnitude of the effect of ξ_t is still minuscule across all maturities, relative to the effect of λ_t. This confirms that the time series of TED spreads are the major channel through which the time variation of λ_t is identified.

Although the long-run component of disaster risk ξ_t has little impact on TED spreads, it has a large impact on interbank rate options. In Panels B and C of Figure 8, we dis-

cover completely opposite patterns. The Black-implied volatilities in both panels are highly sensitive to changes in ξ_t, whereas they are relatively less sensitive to changes in λ_t. Note that the payoffs of caps and swaptions depend on future interbank rates over a long horizon ranging from 1 to 10 years. Hence, the pricing data on caps and swaptions play a critical role in characterizing the time variation of ξ_t.

In sum, our analysis demonstrates that both the short-run and long-run components of disaster risk are well identified using the data on interbank rates and their options. As discussed in Section 2.1, TED spreads do not depend on any risk factors orthogonal to disaster risk and, thus, are highly informative about disaster risk, especially with respect to its short-run component. Furthermore, caps and swaptions are long-term option contracts on future interbank rates, which are pivotal in estimating the long-run component of disaster risk. The benefit of using interbank rate options is not limited to identifying the long-run component: the forward-looking information from caps and swaptions helps us accurately estimate not only the level but also the overall dynamics of disaster risk.

5.4 Implications for the Equity Market

Rare disaster models are often criticized as a macro-finance model with "dark matter." In order to explain the high equity premium and volatility in the postwar period, these models need to rely on the possibility of extremely bad events and its substantial time variation. However, it is not possible to measure disaster risk directly from the data, nor statistically test it with meaningful power, due to the rare nature of such events.

This dark matter criticism raises some concerns about how disaster risk models are calibrated: in typical variable disaster risk models, the dynamics of disaster risk are calibrated to match some key stock market moments, such as the equity premium and the market volatility. However, Chen, Dou, and Kogan (2019) point out that a model with economic

dark matter is likely to be fragile due to the lack of internal refutability and poor out-of-sample performance. Addressing this criticism is challenging: as discussed by Cochrane (2017), it requires either independently anchoring time-varying disaster risk to some data or reconciling multiple asset classes under one consistent assumption about disaster risk.

Our analysis highlights that the interbank market can potentially be useful for addressing the dark matter criticism. We make a plausible assumption that consumption disasters coincide with banking disasters. This identification assumption makes it possible to extract time-varying disaster risk that is manifested in TED spreads as well as caps and swaptions. Since our estimation does not depend on equity market moments, our estimation results essentially serve as an external validity test of disaster risk models for the equity market. The parameter estimates from Section 5.1 suggest that the estimated disaster dynamics are fairly close to those implied by the calibration of Seo and Wachter (2018). Overall, our finding that disaster risk is significant in size and in variation strongly supports a disaster-based explanation of various asset pricing puzzles (Gabaix, 2012; Gourio, 2012; Wachter, 2013).

An additional advantage of our approach is that we obtain the past time series of the short-run and long-run components of disaster risk, namely λ_t and ξ_t. These time series provide an extra basis for testing the implications of disaster risk for the equity market. First of all, Panel A of Table 2 considers the following conditional moments that are associated with the equity market: the price-dividend ratio (log P/D), price-earnings ratio (log P/E), implied variance (IV), expected realized variance (ERV), and variance risk premium (VRP).[11] Since these conditional moments are functions of disaster risk in variable disaster risk models, one testable implication is that their time series variations should be explained by disaster-related state variables.

[11]The price-dividend and price-earnings ratios are downloaded from Robert Shiller's website. The three variance-related variables are downloaded from Hao Zhou's website.

Hence, we regress the five conditional equity market moments on λ_t and ξ_t. We standardize both independent and dependent variables in our regressions to facilitate the interpretation of slope coefficients. In columns (1) and (2) of Panel A, we document that the valuation ratios fall when λ_t and ξ_t rise. For instance, a one standard deviation increase in λ_t leads to a 0.41 standard deviation drop in the log price-dividend ratio. A one standard deviation increase in ξ_t leads to a 0.71 standard deviation drop in the log price-dividend ratio. These negative relations are statistically significant with high Newey and West (1987) t-statistics.[12] These results are consistent with economic intuition as well as empirical evidence: stock market valuations are low in bad economic times with high disaster risk.

In columns (3), (4), and (5), we examine the relation between disaster risk and each of the three variance-related variables. Note that the implied variance and the expected realized variance measure the risk-neutral and physical expectations of future 1-month stock market variance, respectively. The variance risk premium, calculated as their difference, captures compensation for taking variance risk over a 1-month horizon. We expect positive relations from our regression because higher disaster risk results in higher variance risk as well as higher compensation for variance risk. In line with this, we find a strong positive relation between the short-run component of disaster risk λ_t and each variance-related variable. However, we find that the impact of the long-run component ξ_t is insignificant. This is not surprising, since the variance-related variables are based on a very short horizon, namely, a month.

Panel B of Table 2 considers out-of-the money put option prices as additional conditional moments, since they are particularly informative about tail events. At each point in time, we obtain the prices of S&P 500 put options with 90% moneyness, normalized by the underlying index price.[13] This normalization allows us to compare option prices at different points in

[12]Since the sample size is 252, we choose the number of lags to be $0.75\sqrt[3]{252} \simeq 5$, following Newey and West (1994).

[13]We download options data from OptionMetrics. Since we do not observe options with fixed moneyness nor a constant maturity everyday, we use a regression-based interpolation of implied volatilities with respect

time by removing the effect of the index level. Columns (1)-(5) report the results from regressing the normalized prices of put options with 1-, 3-, 6-, 9-, and 12-month maturities on the time series of λ_t and ξ_t.

Column (1) of Panel B demonstrates that λ_t significantly and positively explains the 1-month put option price while ξ_t has no statistically significant impact. This is consistent with the results for the 1-month ahead implied variance in Panel A. Comparing the five columns in Panel B, we can see that λ_t is significant across all maturities. In the case of ξ_t, its economic magnitude and statistical significance gradually increase as option maturity increases. As a result, the effect of ξ_t becomes significant for maturities longer than 6 months. These results are reasonable: the long-run component of disaster risk ξ_t better explains long-horizon equity moments, such as the price-dividend ratio, the price-earnings ratio, and longer-term option prices.

So far, we have examined whether disaster risk can explain the variations in conditional equity market moments. Another testable implication of disaster risk for the equity market is that equity returns should be negatively associated with shocks to λ_t and ξ_t. Panel A of Table 3 reports the results from regressing the market, size, value, momentum, and liquidity factors on changes in λ_t and ξ_t.[14] We find that changes in both the short-run and long-run components of disaster risk are indeed negatively related to the market, size, and liquidity factors. This implies that λ_t and ξ_t capture more than just aggregate market risk. We do not discover any significant results for the value and momentum factors.

Lastly, Panel B of Table 3 investigates how shocks to disaster risk affect contemporaneous excess returns on the Fama-French 10 industry portfolios. Intuitively, some industries are

to moneyness and maturity by adopting the methodology of Seo and Wachter (2019). The price of an option with a specific moneyness and a specific maturity is, then, calculated by plugging the interpolated implied volatility into the Black-Scholes formula.

[14]The market, size, and value factors follow Fama and French (1993), and the momentum factor follows Fama and French (2012). These time series are downloaded from Kenneth French's website. The liquidity risk factor follows Pastor and Stambaugh (2003) and is download from Robert Stambaugh's website.

less sensitive to disaster risk than others. For example, industries that focus on consumer staples, such as food, utilities, energy, and healthcare are likely to be less exposed to disaster risk. This intuition is confirmed in Panel B: the relations between changes in disaster risk and industry returns are statistically insignificant for industries including consumer non-durables, energy, healthcare, and utilities (columns (6)-(9)). In contrast, for industries that are more business-cycle sensitive, such as consumer durables, manufacturing, business equipment, telecommunication, and retail (columns (1)-(5)), we obtain highly significant negative relations.

6 Conclusion

While prior studies on rare disasters calibrate time-varying disaster risk, accurately characterizing it from data remains a considerable challenge. This is extremely difficult because disasters are nearly unobservable events in the post-war sample. In order to tackle this issue, our paper ties time-varying probabilities of disasters to an independent source of data: interbank rates and their options.

Our identification approach relies on the assumption that macroeconomic disasters coincide with banking disasters. This link between banking disasters and the macroeconomy allows us to derive the model-implied TED spreads and prices on interbank rate options as functions of the short-run and long-run components of disaster risk. We show that these data are particularly sensitive to disaster risk, which enables us to reliably infer not only the level of time-varying disaster probabilities but also their dynamics.

The estimation results suggest that disaster risk is significant in size and in variation, strongly upholding the validity of macro-finance models with the rare disaster mechanism. Using the filtered time series of the short-run and long-run components of disaster risk, we also confirm that the implications of these models for equity moments and equity returns

are consistent with the empirical evidence. Put together, we conclude that disaster risk has important implications for the equity market.

In our model, we simply assume that when the interbank market is hit by a large infrequent Poisson shock, the consumption process is also hit by the same shock. This parsimonious setup is sufficient for our estimation and empirical analysis. However, our framework is silent about how macroeconomic and banking disasters arise and how they interact, as we do not model the behaviors of banks nor the structure of the interbank market. We leave this for future work.

Appendix

A Model Derivations

A.1 Risk-Neutral Dynamics

Given the assumption about the pricing kernel in equation (5), the Brownian shocks under the risk-neutral measure are written as follows:

$$\begin{aligned} dB_{c,t}^{Q} &= dB_{c,t} - \theta_c dt, \\ dB_{\lambda,t}^{Q} &= dB_{\lambda,t} - \theta_\lambda \sqrt{\lambda_t} dt, \\ dB_{\xi,t}^{Q} &= dB_{\xi,t} - \theta_\xi \sqrt{\xi_t} dt, \\ dB_{q,t}^{Q} &= dB_{q,t} - \theta_q dt, \end{aligned}$$

where θ_c, θ_λ, θ_ξ, and θ_q indicate the market prices of risk. Moreover, under the risk-neutral measure, the disaster intensity and the moment generating function (MGF) of the jump size distributions are represented as:

$$\begin{aligned} \lambda_t^{Q} &= \lambda_t \Phi_Z(\theta_N, 0), \\ \mathbb{E}^{Q}\left[e^{u_1 Z_c + u_2 Z_q}\right] &= \frac{\Phi_Z(u_1 + \theta_N, u_2)}{\Phi_Z(\theta_N, 0)}, \end{aligned}$$

where $\Phi_Z(u_1, u_2) = \mathbb{E}\left[e^{u_1 Z_c + u_2 Z_q}\right]$ is the MGF of (Z_c, Z_q) under the physical measure.

This leads to the following risk-neutral dynamics of the underlying processes,

$$\begin{aligned}
\frac{dc_t}{c_t} &= \mu_c^Q dt + \sigma_c dB_{c,t}^Q + \left(e^{Z_{c,t}} - 1\right) dN_t, \\
d\lambda_t &= \kappa_\lambda^Q(\nu\xi_t - \lambda_t)dt + \sigma_\lambda\sqrt{\lambda_t}dB_{\lambda,t}^Q, \\
d\xi_t &= \kappa_\xi^Q(\bar{\xi}^Q - \xi_t)dt + \sigma_\xi\sqrt{\xi_t}dB_{\xi,t}^Q, \\
dq_t &= \kappa_q^Q(\bar{q}^Q - q_t)dt + \sigma_q dB_{q,t}^Q + Z_{q,t}dN_t,
\end{aligned}$$

where $\mu_c^Q = \mu_c + \theta_c\sigma_c,\ \kappa_\lambda^Q = \kappa_\lambda - \sigma_\lambda\theta_\lambda,\ \nu = \frac{\kappa_\lambda}{\kappa_\lambda^Q},\ \kappa_\xi^Q = \kappa_\xi - \sigma_\xi\theta_\xi,\ \bar{\xi}^Q = \frac{\kappa_\xi\bar{\xi}}{\kappa_\xi^Q},\ \kappa_q^Q = \kappa_q$, and $\bar{q}^Q = \frac{\kappa_q\bar{q}+\theta_q\sigma_q}{\kappa_q^Q}$.

A.2 Zero-Coupon Rates on Interbank Lending and Government Bonds

The time-t value of \$1 zero-coupon interbank lending maturing at time $t+\tau$ is written as:

$$P_i(t, t+\tau) = \mathbb{E}_t^Q\left[e^{-\int_t^{t+\tau} r_u du}\frac{L_{t+\tau}}{L_t}\right].$$

By multiplying both sides of the above equation with $e^{-\int_0^t r_u du}L_t$, we obtain the following martingale:

$$e^{-\int_0^t r_u du}P_i(t, t+\tau)L_t = \mathbb{E}_t^Q\left[e^{-\int_0^{t+\tau} r_u du}L_{t+\tau}\right].$$

We conjecture that the price of a zero-coupon interbank lending is expressed as:

$$P_i(t, t+\tau) = \exp(a_i(\tau) + b_{i,\lambda}(\tau)\lambda_t + b_{i,\xi}(\tau)\xi_t + b_{i,q}(\tau)q_t).$$

Since $\left(e^{-\int_0^t r_u du}P_{i,t}(\tau)L_t\right)$ is a martingale, the sum of the drift and the jump compensator should be zero. This martingale property provides the system of ordinary differential equa-

tions (ODEs) for a_i, $b_{i,\lambda}$, $b_{i,\xi}$, $b_{i,q}$ as follows:

$$\begin{aligned}
a_i'(\tau) &= -\delta_0 b_{i,\xi}(\tau)\kappa_\xi^Q \bar{\xi}^Q + b_{i,q}(\tau)\kappa_q^Q \bar{q}^Q + \frac{1}{2} b_{i,q}(\tau)^2 \sigma_q^2, \\
b_{i,\lambda}'(\tau) &= -\delta_\lambda - b_{i,\lambda}(\tau)\kappa_\lambda^Q + \frac{1}{2} b_{i,\lambda}(\tau)^2 \sigma_\lambda^2 + \Phi_Z(1+\theta_N, b_{i,q}(\tau)) - \Phi_Z(\theta_N, 0), \\
b_{i,\xi}'(\tau) &= -\delta_\xi + b_{i,\lambda}(\tau)\kappa_\lambda^Q \nu - b_{i,\xi}(\tau)\kappa_\xi^Q + \frac{1}{2} b_{i,\xi}(\tau)^2 \sigma_\xi^2, \\
b_{i,q}'(\tau) &= -\delta_q - b_{i,q}(\tau)\kappa_q^Q,
\end{aligned}$$

with the initial condition: $a_i(0) = b_{i,\lambda}(0) = b_{i,\xi}(0) = b_{i,q}(0) = 0$.

Similarly, the price of a government bond is given as:

$$P_g(t, t+\tau) = \mathbb{E}_t^Q \left[e^{-\int_t^{t+\tau} r_u du} \cdot 1 \right],$$

and we conjecture the price has the form of

$$P_g(t, t+\tau) = \exp(a_g(\tau) + b_{g,\lambda}(\tau)\lambda_t + b_{g,\xi}(\tau)\xi_t + b_{g,q}(\tau) q_t).$$

Since $\left(e^{-\int_0^t r_u du} P_{g,t}(\tau) \right)$ is a martingale, the sum of the drift and the jump compensator should be zero. This martingale property provides the following system of ODEs for a_g, $b_{g,\lambda}$, $b_{g,\xi}$ and $b_{g,q}$:

$$\begin{aligned}
a_g'(\tau) &= -\delta_0 b_{g,\xi}(\tau)\kappa_\xi^Q \bar{\xi}^Q + b_{g,q}(\tau)\kappa_q^Q \bar{q}^Q + \frac{1}{2} b_{g,q}(\tau)^2 \sigma_q^2, \\
b_{g,\lambda}'(\tau) &= -\delta_\lambda - b_{g,\lambda}(\tau)\kappa_\lambda^Q + \frac{1}{2} b_{g,\lambda}(\tau)^2 \sigma_\lambda^2 + \Phi_Z(\theta_N, b_{g,q}(\tau)) - \Phi_Z(\theta_N, 0), \\
b_{g,\xi}'(\tau) &= -\delta_\xi + b_{g,\lambda}(\tau)\kappa_\lambda^Q \nu - b_{g,\xi}(\tau)\kappa_\xi^Q + \frac{1}{2} b_{g,\xi}(\tau)^2 \sigma_\xi^2, \\
b_{g,q}'(\tau) &= -\delta_q - b_{g,q}(\tau)\kappa_q^Q,
\end{aligned}$$

with the initial conditions: $a_g(0) = b_{g,\lambda}(0) = b_{g,\xi}(0) = b_{g,q}(0) = 0$.

Note that $b_{i,q}(\tau)$ and $b_{g,q}(\tau)$ are identical, as their ODEs are identical with the same initial condition. Therefore, we simply denote them as $b_q(\tau)$.

A.3 Cap and Swaption Pricing

Before deriving the expressions for the prices of caps and swaptions, we first find the pricing formula for a put option on $P_i(T_0, T_1)$ with a strike price K. Following Duffie, Pan, and Singleton (2000), Collin-Dufresne and Goldstein (2003), and Trolle and Schwartz (2009), we compute the put option price by using the transform analysis:

$$\begin{aligned}\mathcal{P}(t, T_0, T_1, K) &= \mathbb{E}_t^Q \left[e^{-\int_t^{T_0} r_s ds} (K - P_i(T_0, T_1)) \mathbb{1}_{\{P_i(T_0,T_1) < K\}} \right] \\ &= K G_{0,1}(\log K) - G_{1,1}(\log K),\end{aligned}$$

where

$$\begin{aligned}G_{a,b}(y) &= \frac{\psi(a, t, T_0, T_1)}{2} - \frac{1}{\pi} \int_0^\infty \frac{\mathrm{Im}\left[\psi(a + iub, t, T_0, T_1) e^{-iuy}\right]}{u} du, \\ \psi(u, t, T_0, T_1) &= \mathbb{E}_t^Q \left[\exp\left(- \int_t^{T_0} r_s ds \right) e^{u \log(P_i(T_0,T_1))} \right].\end{aligned}$$

Note that $\psi(\cdot)$ solves the complex-valued ODEs of Duffie, Pan, and Singleton (2000), and $\mathrm{Im}(\cdot)$ represents the imaginary part of a complex number.

The time-t cap price is given by equation (12). Under the approximation $e^{-\int_{t_j}^{t_{j+1}} r_s ds} \approx P_i(t_j, t_{j+1})$, we re-express the cap pricing formula as:

$$\begin{aligned}V_{\text{cap}}^{(T)}(t, K_c) &\approx \sum_{j=1}^{m_T} \mathbb{E}_t^Q \left[\exp\left(- \int_t^{t_j} r_s ds \right) P_i(t_j, t_{j+1}) \left[\frac{1}{P_i(t_j, t_{j+1})} - 1 - \Delta \times K_c \right]^+ \right] \\ &= (1 + \Delta \times K_c) \sum_{j=1}^{m_T} \mathcal{P}\left(t, t_j, t_{j+1}, \frac{1}{1 + \Delta \times K_c} \right). \qquad \text{(A.1)}\end{aligned}$$

As discussed in Section 2.3, we price swaptions by adopting the stochastic duration method suggested by Wei (1997), Munk (1999), and Trolle and Schwartz (2009). Applying this method to equation (14) results in:

$$\begin{aligned} V_{\text{pay}}^{(T,\bar{T})}(t,K_s) &= \mathbb{E}_t^Q\left[\exp\left(-\int_t^{t+T} r_s ds\right)\left[1-V_{\text{fixed}}^{(\bar{T})}(t+T,K_s)\right]^+\right] \\ &\approx \zeta\mathcal{P}(t,T,t+\mathcal{D}(t,T,\bar{T}),\zeta^{-1}), \end{aligned} \tag{A.2}$$

where $\zeta = \frac{\sum_{l=1}^{\bar{T}/\Delta} Y_l P_i(t,t+T+l\Delta)}{P_i(t,t+\mathcal{D}(t,T,\bar{T}))}$. The stochastic duration $\mathcal{D}(t,T,\bar{T})$, or simply $\mathcal{D}(t)$, is defined as a quantity that satisfies:

$$\begin{aligned} &b_{i,\lambda}(\mathcal{D}(t))^2\sigma_\lambda^2\lambda_t + b_{i,\xi}(\mathcal{D}(t))^2\sigma_\xi^2\xi_t + b_q(\mathcal{D}(t))^2\sigma_q^2 + [\Phi(\theta_N, 2b_q(\mathcal{D}(t))) - 2\Phi(\theta_N, b_q(\mathcal{D}(t))) + \Phi(\theta_N,0)]\,\lambda_t \\ &= \left[\sum_{j=1}^{\bar{T}/\Delta} w_j b_{i,\lambda}(T+j\Delta)\right]^2\sigma_\lambda^2\lambda_t + \left[\sum_{j=1}^{\bar{T}/\Delta} w_j b_{i,\xi}(T+j\Delta)\right]^2\sigma_\xi^2\xi_t + \left[\sum_{j=1}^{\bar{T}/\Delta} w_j b_q(T+j\Delta)\right]^2\sigma_q^2 \\ &\quad + \left[\sum_{j=1}^{\bar{T}/\Delta}\left[w_j^2\Phi(\theta_N, 2b_q(T+j\Delta)) - 2w_j\Phi(\theta_N, b_q(T+j\Delta))\right.\right. \\ &\quad \left.\left. + \sum_{k>j} 2w_j w_k \Phi(\theta_N, b_q(T+j\Delta) + b_q(T+k\Delta))\right] + \Phi(\theta_N,0)\right]\lambda_t, \end{aligned} \tag{A.3}$$

where $w_j = \frac{Y_j P_i(t,t+T+j\Delta)}{\sum_{l=1}^{\bar{T}/\Delta} Y_l P_i(t,t+T+l\Delta)}$, $Y_j = \Delta \times K_s$ for $j = 1,\ 2,\ \cdots,\ \frac{\bar{T}}{\Delta} - 1$, and $Y_{\bar{T}/\Delta} = 1 + \Delta \times K_s$.

B The Extended Kalman Filter

As discussed in Section 4, we derive the discrete-time state equation based on the exact relation between $S_t = [\lambda_t, \xi_t]^\top$ and $S_{t-\Delta t} = [\lambda_{t-\Delta t}, \xi_{t-\Delta t}]^\top$. To do so, we first integrate both

sides of the stochastic differential equations for λ_t and ξ_t from time $t-\Delta t$ to time t:

$$\begin{aligned}
\lambda_t &= \lambda_{t-\Delta t} + \kappa_\lambda \int_{t-\Delta t}^{t} (\xi_u - \lambda_u) du + \sigma_\lambda \int_{t-\Delta t}^{t} \sqrt{\lambda_u} dB_{\lambda,u}, \\
\xi_t &= \xi_{t-\Delta t} + \kappa_\xi \int_{t-\Delta t}^{t} (\bar{\xi} - \xi_u) du + \sigma_\xi \int_{t-\Delta t}^{t} \sqrt{\xi_u} dB_{\xi,u}.
\end{aligned}$$

Note that an Ito integral is a martingale and, hence, its conditional mean is zero. By taking the conditional expectations $\mathbb{E}_{t-\Delta t}[\cdot]$ on both sides of the equations, we simply obtain $\mathbb{E}_{t-\Delta t}[S_t] = \eta + \Psi S_{t-\Delta t}$, where

$$\begin{aligned}
\eta &= \begin{bmatrix} -\frac{\kappa_\lambda \bar{\xi}}{\kappa_\lambda - \kappa_\xi}\left(e^{-\kappa_\xi \Delta t} - e^{-\kappa_\lambda \Delta t}\right) + \bar{\xi}\left(1 - e^{-\kappa_\lambda \Delta t}\right) \\ \bar{\xi}\left(1 - e^{-\kappa_\xi \Delta t}\right) \end{bmatrix}, \\
\Psi &= \begin{bmatrix} e^{-\kappa_\lambda \Delta t} & \frac{\kappa_\lambda}{\kappa_\lambda - \kappa_\xi}\left(e^{-\kappa_\xi \Delta t} - e^{-\kappa_\lambda \Delta t}\right) \\ 0 & e^{-\kappa_\xi \Delta t} \end{bmatrix}.
\end{aligned}$$

This relation allows us to express S_t as in equation (16):

$$S_t = \mathbb{E}_{t-\Delta t}[S_t] + \epsilon_t, \quad \text{where } \mathbb{E}_{t-\Delta t}[\epsilon_t] = 0 \text{ and } \mathrm{Var}_{t-\Delta t}[\epsilon_t] = \Omega_{t-\Delta t},$$

where the 2×2 covariance matrix $\Omega_{t-\Delta t}$ is given by

$$\Omega_{t-\Delta t} = \begin{bmatrix} \Omega_{\lambda\lambda,t-\Delta t} & \Omega_{\lambda\xi,t-\Delta t} \\ \Omega_{\lambda\xi,t-\Delta t} & \Omega_{\xi\xi,t-\Delta t} \end{bmatrix}.$$

Clearly, ϵ_t is non-normal. However, in order to use a conventional filtering approach, we approximate it by a mean-zero normal random variable with the same covariance matrix $\Omega_{t-\Delta t}$.[15] We find each element of $\Omega_{t-\Delta t}$ by considering the marginal and joint dynamics of

[15] As discussed in Section 4, it is well known that the effect of this approximation is minimal.

λ_t and ξ_t:

$$
\begin{aligned}
\Omega_{\lambda\lambda,t-\Delta t} &= \frac{\kappa_\lambda^2\sigma_\xi^2\xi_{t-\Delta t}}{(\kappa_\lambda-\kappa_\xi)^2\kappa_\xi}\left(e^{-\kappa_\xi\Delta t}-e^{-2\kappa_\xi\Delta t}\right)+\frac{\kappa_\lambda^2\bar{\xi}\sigma_\xi^2}{2(\kappa_\lambda-\kappa_\xi)^2\kappa_\xi}\left(1-e^{-\kappa_\xi\Delta t}\right)^2 \\
&\quad-\frac{2\kappa_\lambda\sigma_\xi^2(\xi_{t-\Delta t}-\bar{\xi})}{(\kappa_\lambda-\kappa_\xi)^2}\left(e^{-\kappa_\xi\Delta t}-e^{-(\kappa_\lambda+\kappa_\xi)\Delta t}\right)-\frac{2\kappa_\lambda^2\sigma_\xi^2\bar{\xi}}{(\kappa_\lambda-\kappa_\xi)^2(\kappa_\xi+\kappa_\lambda)}\left(1-e^{-(\kappa_\lambda+\kappa_\xi)\Delta t}\right) \\
&\quad+\frac{\kappa_\lambda^2\sigma_\xi^2(\xi_{t-\Delta t}-\bar{\xi})}{(\kappa_\lambda-\kappa_\xi)^2(2\kappa_\lambda-\kappa_\xi)}\left(e^{-\kappa_\xi\Delta t}-e^{-2\kappa_\lambda\Delta t}\right)+\frac{\kappa_\lambda\sigma_\xi^2\bar{\xi}}{2(\kappa_\lambda-\kappa_\xi)^2}\left(1-e^{-2\kappa_\lambda\Delta t}\right) \\
&\quad+\frac{(\lambda_{t-\Delta t}-\bar{\xi})\sigma_\lambda^2}{\kappa_\lambda}\left(e^{-\kappa_\lambda\Delta t}-e^{-2\kappa_\lambda\Delta t}\right)+\frac{\kappa_\lambda(\xi_{t-\Delta t}-\bar{\xi})\sigma_\lambda^2}{(\kappa_\lambda-\kappa_\xi)(2\kappa_\lambda-\kappa_\xi)}\left(e^{-\kappa_\xi\Delta t}-e^{-2\kappa_\lambda\Delta t}\right) \\
&\quad-\frac{(\xi_{t-\Delta t}-\bar{\xi})\sigma_\lambda^2}{\kappa_\lambda-\kappa_\xi}\left(e^{-\kappa_\lambda\Delta t}-e^{-2\kappa_\lambda\Delta t}\right)+\frac{\bar{\xi}\sigma_\lambda^2}{2\kappa_\lambda}\left(1-e^{-2\kappa_\lambda\Delta t}\right), \\
\Omega_{\xi\xi,t-\Delta t} &= \frac{\sigma_\xi^2\xi_{t-\Delta t}}{\kappa_\xi}\left(e^{-\kappa_\xi\Delta t}-e^{-2\kappa_\xi\Delta t}\right)+\frac{\sigma_\xi^2\bar{\xi}}{2\kappa_\xi}\left(1-e^{-\kappa_\xi\Delta t}\right)^2, \\
\Omega_{\lambda\xi,t-\Delta t} &= \frac{\kappa_\lambda}{\kappa_\lambda-\kappa_\xi}\Omega_{\xi\xi,t-\Delta t} \\
&\quad-\frac{\sigma_\xi^2\left(\xi_{t-\Delta t}-\bar{\xi}\right)}{\kappa_\lambda-\kappa_\xi}\left(e^{-\kappa_\xi\Delta t}-e^{-(\kappa_\lambda+\kappa_\xi)\Delta t}\right)-\frac{\kappa_\lambda\sigma_\xi^2\bar{\xi}}{(\kappa_\lambda-\kappa_\xi)(\kappa_\lambda+\kappa_\xi)}\left(1-e^{-(\kappa_\xi+\kappa_\lambda)\Delta t}\right).
\end{aligned}
$$

Since our measurement equation is not linear in the state variables, we adopt the extended Kalman filter. Specifically, we locally linearize the function $h(S,q)$ in equation (17) as follows:

$$
h(S_t,q_t)\approx h\left(\hat{S}_{t|t-\Delta t},q_t\right)+H_t\times\left(S_t-\hat{S}_{t|t-\Delta t}\right),
$$

where $\hat{S}_{t|t-\Delta t}$ is the predicted time-t state vector given the information at time $t-\Delta t$, and $H_t=\frac{\partial h}{\partial S}\left(\hat{S}_{t|t-\Delta t},q_t\right)$ is the partial derivative of $h(S,q)$ with respect to S, evaluated at the point $(\hat{S}_{t|t-\Delta t},\ q_t)$.

Then, according to the Kalman filter recursion, we obtain the filtered state vector at time

t (i.e. $\hat{S}_t$) from the filtered state vector at time $t - \Delta t$ (i.e. $\hat{S}_{t-\Delta t}$) as follows:

$$\begin{aligned}
\hat{S}_{t|t-\Delta t} &= \eta + \Psi \hat{S}_{t-\Delta t}, \\
P_{t|t-\Delta t} &= \Psi P_{t-\Delta t} \Psi' + \Omega_{t-\Delta t}, \\
\hat{S}_t &= \hat{S}_{t|t-\Delta t} + K_t \hat{e}_t, \\
P_t &= P_{t|t-\Delta t} - K_t H_t P_{t|t-\Delta t},
\end{aligned}$$

where

$$\begin{aligned}
K_t &= P_{t|t-\Delta t} H_t' F_t^{-1}, \\
F_t &= H_t P_{t|t-\Delta t} H_t' + Q, \\
\hat{e}_t &= Y_t - h\left(\hat{S}_{t|t-\Delta t}, q_t\right).
\end{aligned}$$

For the initial month, the values of $\hat{S}_{t-\Delta t}$ and $P_{t-\Delta t}$ are set to be the unconditional mean and variance of S_t. The Kalman filter recursion also enables us to calculate the likelihood of observing Y_t conditional on $Y_{t-\Delta t}$:

$$\log \mathcal{L}_t = -\frac{l}{2} \log(2\pi) - \frac{1}{2} \log |F_t| - \frac{1}{2} \hat{e}_t' F_t^{-1} \hat{e}_t,$$

where l is the size of the vector Y_t.

References

Adrian, Tobias, Erkko Etula, and Tyler Muir, 2014, Financial intermediaries and the cross-section of asset returns, *The Journal of Finance* 69, 2557–2596.

Allen, Linda, Turan G. Bali, and Yi Tang, 2012, Does systemic risk in the financial sector predict future economic downturns?, *The Review of Financial Studies* 25, 3000–3036.

Ang, Andrew, and Monika Piazzesi, 2003, A no-arbitrage vector autoregression of term structure dynamics with macroeconomic and latent variables, *Journal of Monetary Economics* 50, 745–787.

Barro, Robert J., 2006, Rare disasters and asset markets in the twentieth century, *Quarterly Journal of Economics* 121, 823–866.

Barro, Robert J., and José F. Ursúa, 2008, Macroeconomic crises since 1870, *Brookings Papers on Economic Activity* no. 1, 255–350.

Berkman, Henk, Ben Jacobsen, and John B. Lee, 2011, Time-varying rare disaster risk and stock returns, *Journal of Financial Economics* 101, 313–332.

Bernanke, Ben S., 1983, Nonmonetary effects of the financial crisis in the propagation of the Great Depression, *The American Economic Review* 73, 257–276.

Black, Fischer, 1976, The pricing of commodity contracts, *Journal of Financial Economics* 3, 167–179.

Brunnermeier, Markus K., and Yuliy Sannikov, 2014, A macroeconomic model with a financial sector, *American Economic Review* 104, 379–421.

Chen, Hui, Winston Dou, and Leonid Kogan, 2019, Measuring the "dark matter" in asset pricing models, The Rodney L. White Center Working Papers Series at the Wharton School.

Chen, Ren-Raw, and Louis Scott, 2003, Multi-factor Cox-Ingersoll-Ross models of the term structure: Estimates and tests from a Kalman filter model, *The Journal of Real Estate Finance and Economics* 27, 143–172.

Cochrane, John H., 2017, Macro-finance, *Review of Finance* 21, 945–985.

Collin-Dufresne, Pierre, and Robert Goldstein, 2003, Generalizing the affine framework to HJM and random field models, *Working paper*.

Duan, Jin-Chuan, and Jean-Guy Simonato, 1999, Estimating and testing exponential-affine term structure models by Kalman filter, *Review of Quantitative Finance and Accounting* 13, 111–135.

Duffee, Gregory R, 1999, Estimating the price of default risk, *Review of Financial Studies* 12, 197–226.

Duffie, Darrell, Jun Pan, and Kenneth Singleton, 2000, Transform analysis and asset pricing for affine jump-diffusions, *Econometrica* 68, 1343–1376.

Fama, Eugene F., and Kenneth R. French, 1993, Common risk factors in the returns on bonds and stocks, *Journal of Financial Economics* 33, 3–56.

Fama, Eugene F., and Kenneth R. French, 2012, Size, value, and momentum in international stock returns, *Journal of financial economics* 105, 457–472.

Filipović, Damir, and Anders B. Trolle, 2013, The term structure of interbank risk, *Journal of Financial Economics* 109, 707–733.

Gabaix, Xavier, 2012, An exactly solved framework for ten puzzles in macro-finance, *Quarterly Journal of Economics* 127, 645–700.

Giesecke, Kay, Francis A. Longstaff, Stephen Schaefer, and Ilya A. Strebulaev, 2014, Macroeconomic effects of corporate default crisis: A long-term perspective, *Journal of Financial Economics* 111, 297–310.

Gourio, François, 2012, Disaster risk and business cycles, *American Economic Review* 102, 2734–2766.

Han, Bing, 2007, Stochastic volatilities and correlations of bond yields, *The Journal of Finance* 62, 1491–1524.

He, Zhiguo, Bryan Kelly, and Asaf Manela, 2017, Intermediary asset pricing: New evidence from many asset classes, *Journal of Financial Economics* 126, 1–35.

He, Zhiguo, and Arvind Krishnamurthy, 2013, Intermediary asset pricing, *American Economic Review* 103, 732–70.

Joslin, Scott, Anh Le, and Kenneth J. Singleton, 2013, Why Gaussian macro-finance term structure models are (nearly) unconstrained factor-VARs, *Journal of Financial Economics* 109, 604–622.

Longstaff, Francis A., Pedro Santa-Clara, and Eduardo S. Schwartz, 2001, The relative valuation of caps and swaptions: Theory and empirical evidence, *The Journal of Finance* 56, 2067–2109.

Manela, Asaf, and Alan Moreira, 2017, News implied volatility and disaster concerns, *Journal of Financial Economics* 123, 137–162.

McAndrews, James, Asani Sarkar, and Zhenyu Wang, 2017, The effect of the term auction facility on the London interbank offered rate, *Journal of Banking & Finance* 83, 135–152.

Michaud, François-Louis, and Christian Upper, 2008, What drives interbank rates? Evidence from the Libor panel, *BIS Quarterly Review*.

Munk, Claus, 1999, Stochastic duration and fast coupon bond option pricing in multi-factor models, *Review of Derivatives Research* 3, 157–181.

Nelson, Charles R., and Andrew F. Siegel, 1987, Parsimonious modeling of yield curves, *Journal of business* pp. 473–489.

Newey, Whitney, and Kenneth West, 1987, A simple, positive semi-definite, heteroskedasticity and autocorrelation consistent covariance matrix, *Econometrica* 55, 703–708.

Newey, Whitney K., and Kenneth D. West, 1994, Automatic lag selection in covariance matrix estimation, *Review of Economic Studies* 61, 631–653.

Pastor, Lubos, and Robert F. Stambaugh, 2003, Liquidity risk and expected stock returns, *Journal of Political Economy* 111, 642–685.

Reinhart, Carmen M., and Kenneth S. Rogoff, 2013, Banking crises: an equal opportunity menace, *Journal of Banking & Finance* 37, 4557–4573.

Rietz, Thomas A., 1988, The equity risk premium: A solution, *Journal of Monetary Economics* 22, 117–131.

Seo, Sang Byung, and Jessica A Wachter, 2018, Do rare events explain CDX tranche spreads?, *The Journal of Finance* 73, 2343–2383.

Seo, Sang Byung, and Jessica A. Wachter, 2019, Option prices in a model with stochastic disaster risk, *Management Science* 65, 3449–3469.

Taylor, John B., and John C. Williams, 2009, A black swan in the money market, *American Economic Journal: Macroeconomics* 1, 58–83.

Trolle, Anders B., and Eduardo S. Schwartz, 2009, Unspanned stochastic volatility and the pricing of commodity derivatives, *The Review of Financial Studies* 22, 4423–4461.

Tsai, Jerry, 2015, Rare disasters and the term structure of interest rates, Working paper.

Tsai, Jerry, and Jessica A. Wachter, 2015, Disaster risk and its implications for asset pricing, *Annual Review of Financial Economics* 7, 219–252.

Wachter, Jessica A., 2013, Can time-varying risk of rare disasters explain aggregate stock market volatility?, *Journal of Finance* 68, 987–1035.

Wei, Jason Z., 1997, A simple approach to bond option pricing, *Journal of Futures Markets: Futures, Options, and Other Derivative Products* 17, 131–160.

Table 1: Parameter Estimates

Consumption growth	μ_c	σ_c		
	0.0138	0.0081		
	(0.0018)	(0.0005)		
Expected inflation	κ_q	σ_q	$\bar{q}$	
	0.5072	0.0062	0.0206	
	(0.2773)	(0.0010)	(0.0028)	
Disaster risk	κ_λ	σ_λ		
	0.1861	0.1423		
	(0.0024)	(0.0010)		
	κ_ξ	σ_ξ	$\bar{\xi}$	
	0.0750	0.0240	0.0239	
	(0.0009)	(0.0004)	(0.0006)	
Risk-free rate	δ_λ	δ_ξ	δ_q	δ_0
	-0.1679	-2.3764	0.9524	0.0602
	(0.0040)	(0.0325)	(0.0086)	
Market price of risk	θ_λ	θ_ξ	θ_q	θ_N
	0.1950	0.9044	2.1387	-0.1640
	(0.0036)	(0.0157)	(0.0330)	(0.0021)
Measurement errors	σ_{SP}	σ_{ITR}	σ_{OPT}	
	0.0014	0.0050	0.0664	
	(0.0000)	(0.0000)	(0.0008)	

Notes: This table reports the values of the model parameters estimated through the extended Kalman filter/MLE procedure. The model consists of the following four state variables: real consumption (c_t), expected inflation (q_t), instantaneous disaster intensity (λ_t), and its long-run component (ξ_t). We also report the risk-free rate factor loadings and the market prices of risk. Lastly reported are the standard deviations of measurement errors, where subscripts SP, ITR, and OPT indicate TED spreads, interest rates, and Black-implied volatilities, respectively.

Table 2: Disaster Risk and Conditional Equity Moments

Panel A: Valuation ratios and variance-related variables					
	(1)	(2)	(3)	(4)	(5)
	log P/D	log P/E	IV	ERV	VRP
λ_t	-0.41	-0.27	0.58	0.57	0.25
	[-3.95]	[-2.55]	[3.25]	[2.84]	[1.91]
ξ_t	-0.71	-0.75	-0.02	0.06	-0.10
	[-6.81]	[-7.72]	[-0.25]	[0.86]	[-1.52]
Adj R^2 (%)	60.12	58.53	34.15	32.18	7.58
Panel B: Out-of-the-money put option prices					
	(1)	(2)	(3)	(4)	(5)
	1 month	3 months	6 months	9 months	12 months
λ_t	0.56	0.57	0.57	0.50	0.32
	[3.14]	[3.87]	[4.22]	[3.92]	[2.93]
ξ_t	0.02	0.06	0.15	0.23	0.22
	[0.27]	[0.72]	[1.66]	[2.44]	[2.18]
Adj R^2 (%)	30.48	31.28	32.62	27.36	12.90

Notes: This table reports the results of contemporaneous time series regressions that examine the relation between the filtered disaster risk variables (λ_t and ξ_t) and conditional equity market moments. In both panels, we standardize the independent and dependent variables. In Panel A, the dependent variables are the log price-dividend ratio (log P/D), log price-earnings ratio (log P/E), implied variance (IV), expected realized variance (ERV), and the variance risk premium (VRP). In Panel B, the dependent variables are the normalized put prices of 90% moneyness put options with 1-, 3-, 6-, 9- and 12-month maturities. The t-statistics are reported in brackets and are computed based on the Newey and West (1987) method with five lags.

Table 3: Shocks to Disaster Risk and Equity Returns

Panel A: Factor portfolios					
	(1)	(2)	(3)	(4)	(5)
	MktRf	SMB	HML	MOM	LIQ
$\Delta\lambda_t$	-0.14	-0.10	0.09	0.00	-0.18
	[-2.59]	[-2.08]	[1.18]	[0.03]	[-2.17]
$\Delta\xi_t$	-0.22	-0.13	0.00	0.10	-0.13
	[-2.76]	[-2.86]	[-0.01]	[1.25]	[-1.59]
Adj R^2 (%)	6.29	2.36	0.49	0.54	4.51
Panel B: Fama-French 10 industry portfolios					
	(1)	(2)	(3)	(4)	(5)
	Durbl	Manuf	HiTec	Telcm	Shops
$\Delta\lambda_t$	-0.12	-0.14	-0.13	-0.14	-0.08
	[-2.49]	[-2.15]	[-2.65]	[-2.66]	[-2.08]
$\Delta\xi_t$	-0.20	-0.20	-0.23	-0.18	-0.20
	[-3.07]	[-2.78]	[-2.92]	[-2.11]	[-2.72]
Adj R^2 (%)	5.00	5.49	6.53	4.98	4.01
	(6)	(7)	(8)	(9)	(10)
	NoDur	Enrgy	Hlth	Utils	Other
$\Delta\lambda_t$	-0.04	-0.10	-0.08	-0.11	-0.08
	[-0.83]	[-1.64]	[-1.37]	[-1.51]	[-1.55]
$\Delta\xi_t$	-0.04	-0.10	-0.12	0.02	-0.20
	[-0.53]	[-1.47]	[-1.58]	[0.21]	[-2.74]
Adj R^2 (%)	-0.09	1.53	1.57	0.88	4.37

Notes: This table reports the results of contemporaneous time series regressions that examine the relation between changes in the filtered disaster risk variables (λ_t and ξ_t) and equity returns. In both panels, we standardize the independent and dependent variables. In Panel A, the dependent variables are the excess market return (MktRf), size factor return (SMB), book-to-market factor return (HML), momentum factor return (MOM), and liquidity factor return (LIQ). In Panel B, the dependent variables are the excess returns on the 10 Fama-French industry portfolios. These industries include consumer durables (Durbl), manufacturing (Manuf), business equipment (HiTec), telecommunication (Telcm), retail (Shops), consumer non-durables (NoDur), energy (Enrgy), healthcare (Hlth), utilities (Utils), and others (Other). The t-statistics are reported in brackets and are computed based on the Newey and West (1987) method with five lags.

Figure 1: Size Distributions of Consumption Declines and Inflation Rates During Disasters

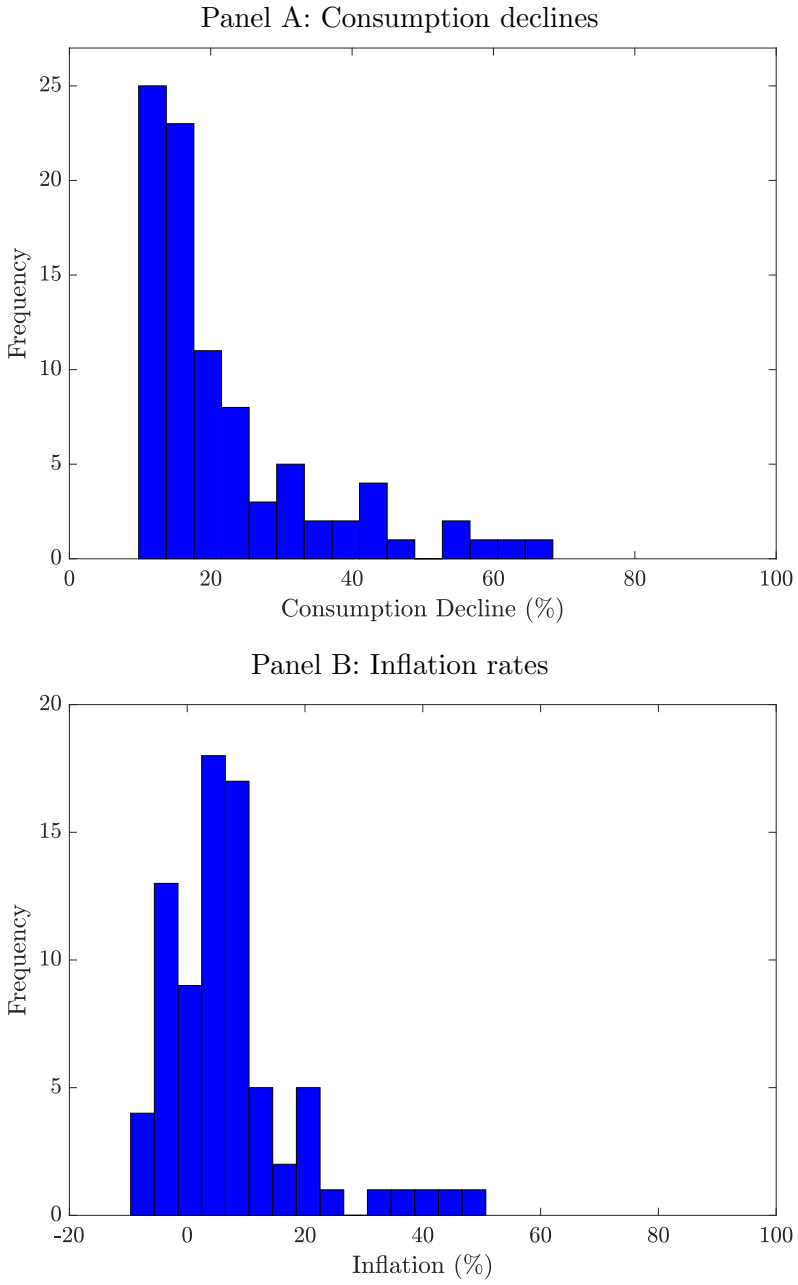

Notes: This figure shows the empirical distribution of consumption declines (Panel A) and the empirical distribution of inflation rates during consumption disasters (Panel B), both obtained from the Barro and Ursúa (2008) dataset. In Panel B, we remove extreme hyperinflation events by excluding the observations that fall more than 3 times the interquartile range above the third quartile. No observations fall more than 3 times the interquartile range below the first quartile.

Figure 2: Interest rates and the TED spread in the Data and in the Model

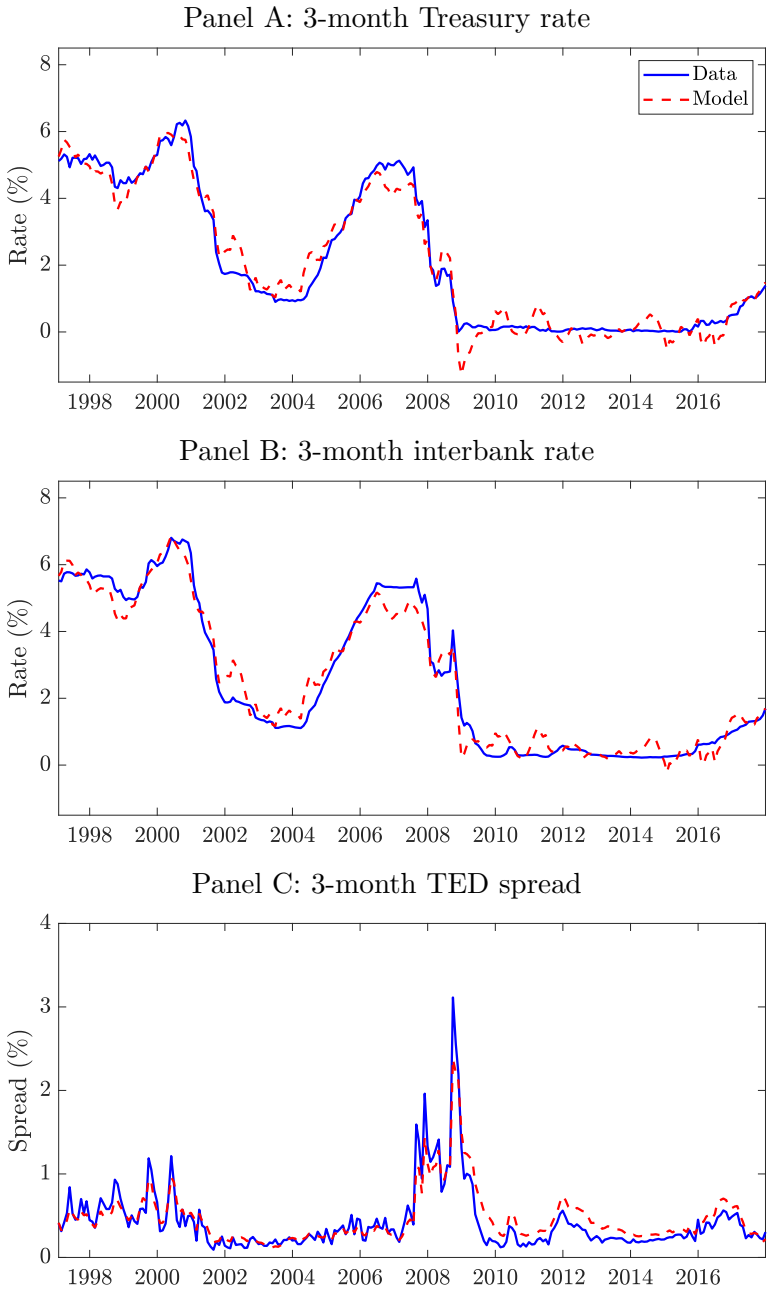

Notes: This figure plots the time series of the Treasury rate (Panel A), the interbank rate (Panel B), and the TED spread (Panel C) with a 3-month maturity in the data and in the model, from January 1997 to December 2017. The solid blue lines represent the data and the dashed red lines represent the model. All values are expressed in percentage terms.

Figure 3: Interest Rates in the Data and in the Model

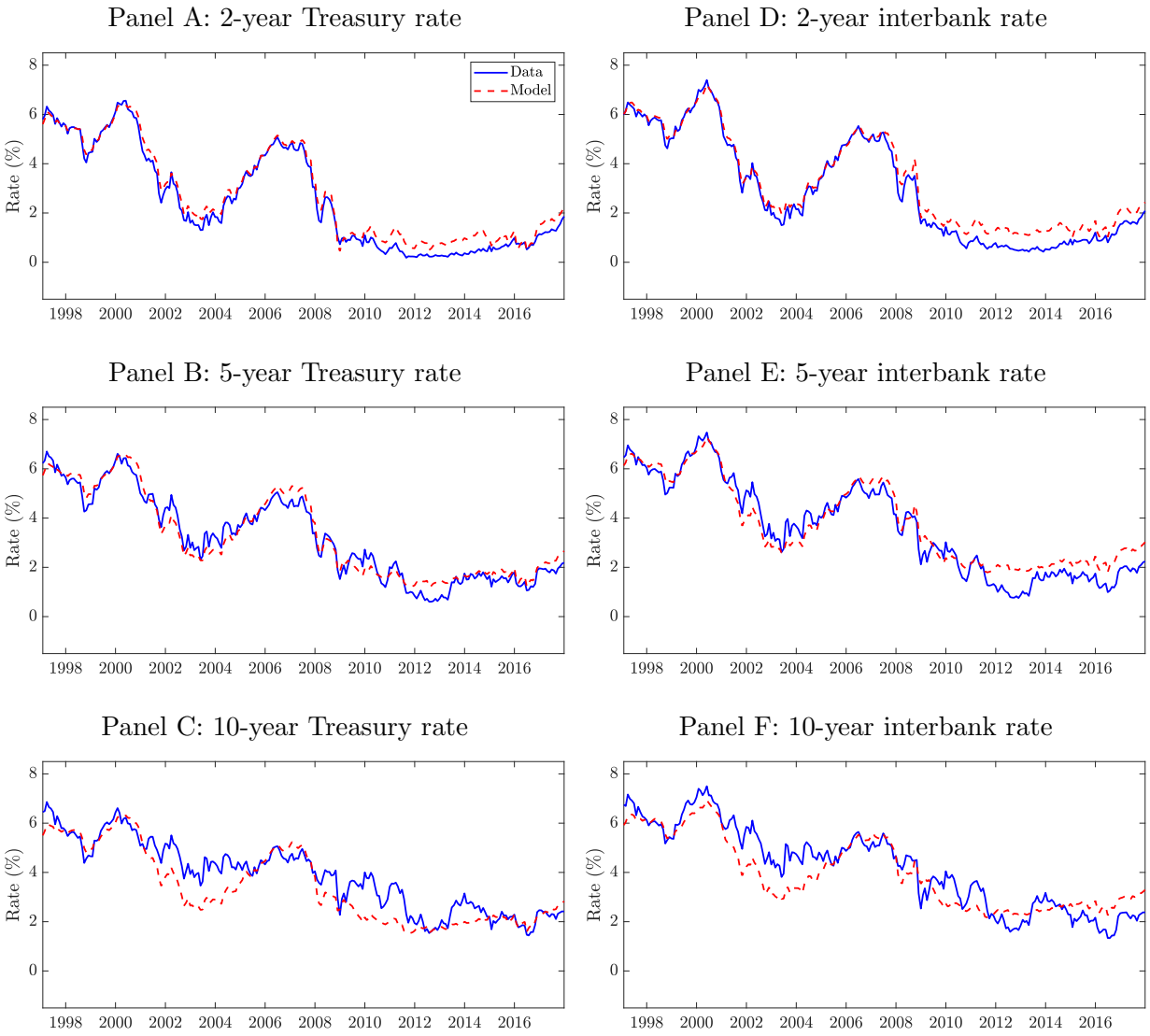

Notes: This figure depicts the time series of the Treasury rates (Panels A, B, and C) and the interbank rates (Panels D, E, and F) with 2-, 5-, and 10-year maturities in the data and in the model, from January 1997 to December 2017. The solid blue lines represent the data, and the dashed red lines represent the model. All values are expressed in percentage terms.

Figure 4: Black-Implied Volatilities in the Data and in the Model

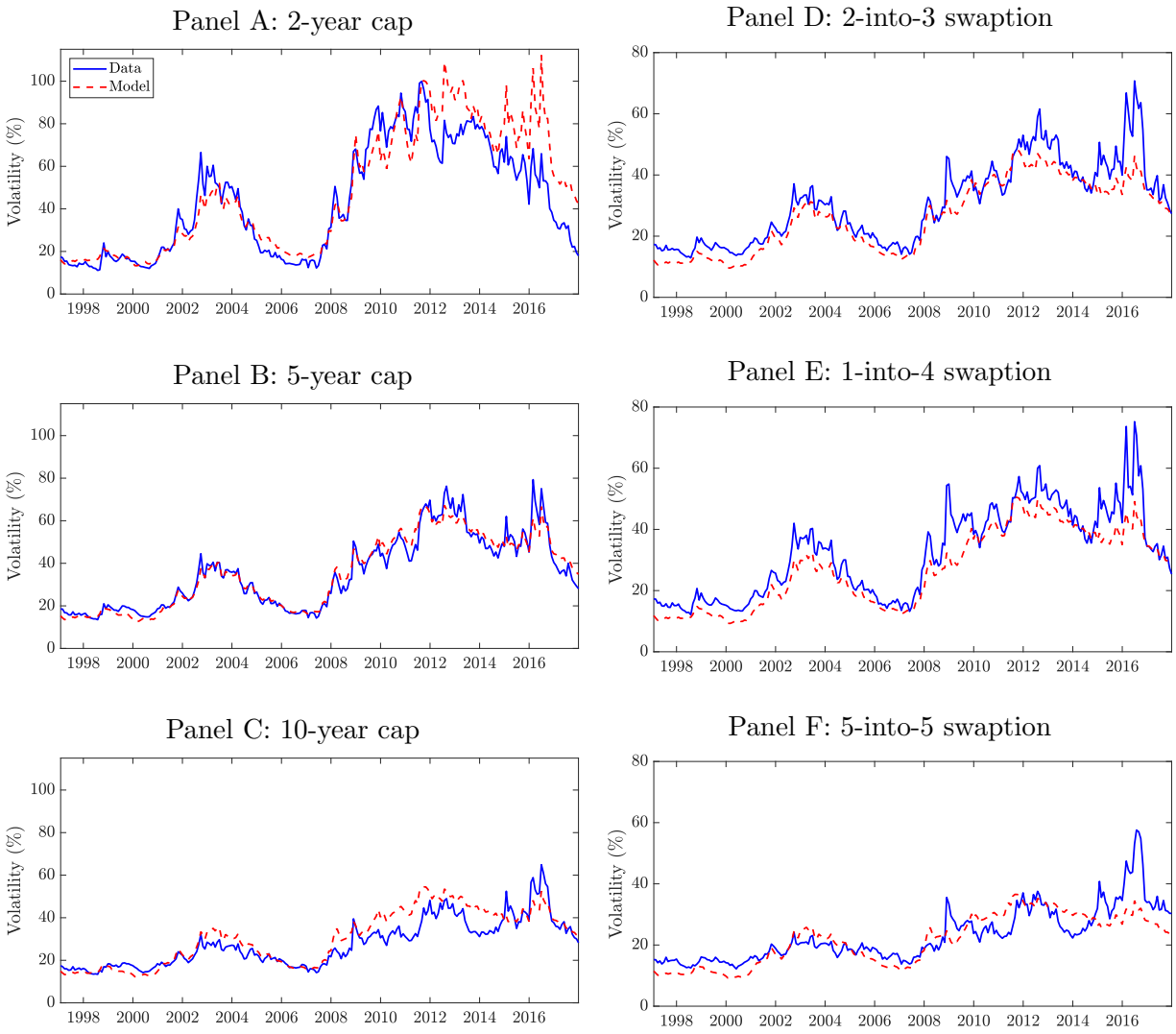

Notes: This figure presents the time series of the Black-implied volatilities for the 2-, 5-, and 10-year caps (Panels A, B, and C), and those for the 2-into-3, 1-into-4, and 5-into-5 swaptions (Panels D, E, and F) in the data and in the model, from January 1997 to December 2017. The solid blue lines represent the data, and the dashed red lines represent the model. All values are expressed in percentage terms.

Figure 5: A Comparison Between the 1M-Into-10Y Swaption Volatility and the TYVIX

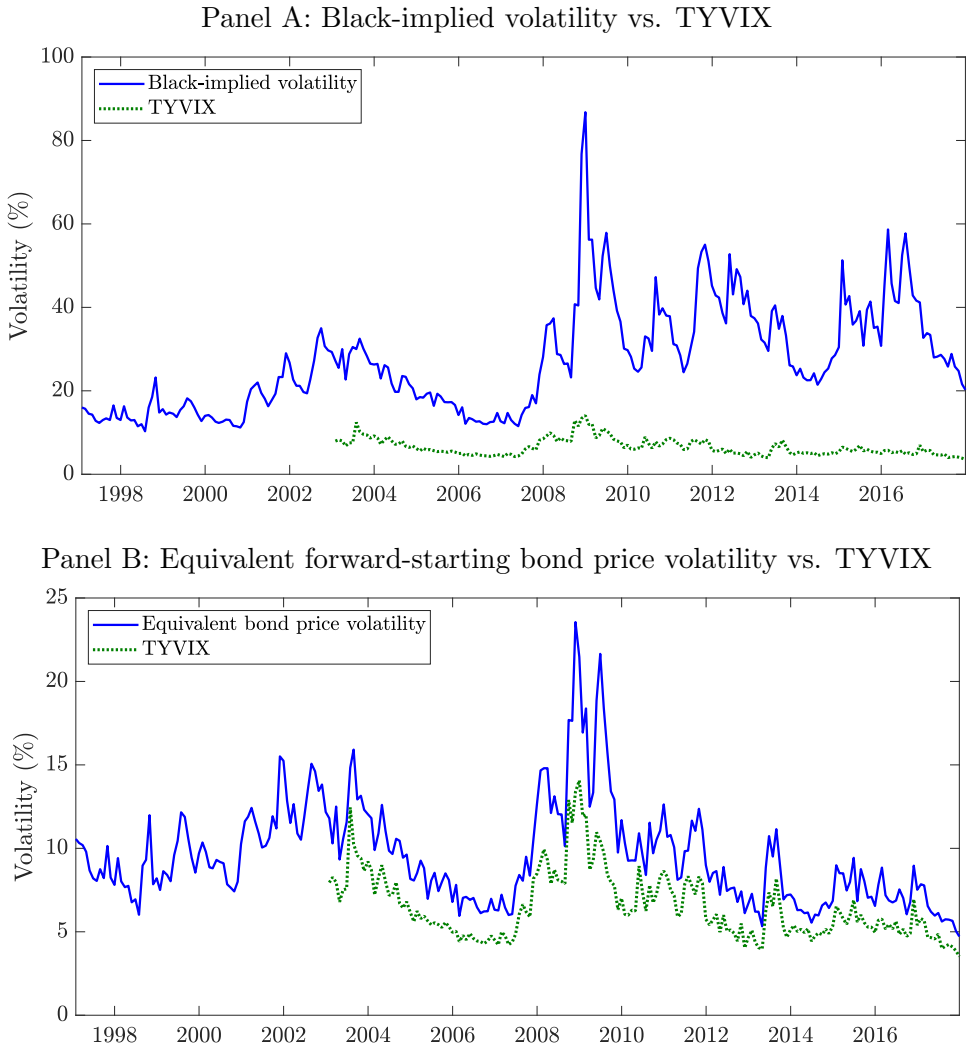

Notes: This figure compares the time series of the 1-month-into-10-year swaption Black-implied volatility (Panel A) and the equivalent bond price volatility (Panel B) with the TYVIX in the data. The swaption-implied volatilities are from January 1997 to December 2017, whereas the TYVIX is available from January 2003. The solid blue lines represent the swaption-implied volatilities, and the dotted green lines represent the TYVIX. All values are expressed in percentage terms.

Figure 6: Equivalent Bond Price Volatilities in the Data and in the Model

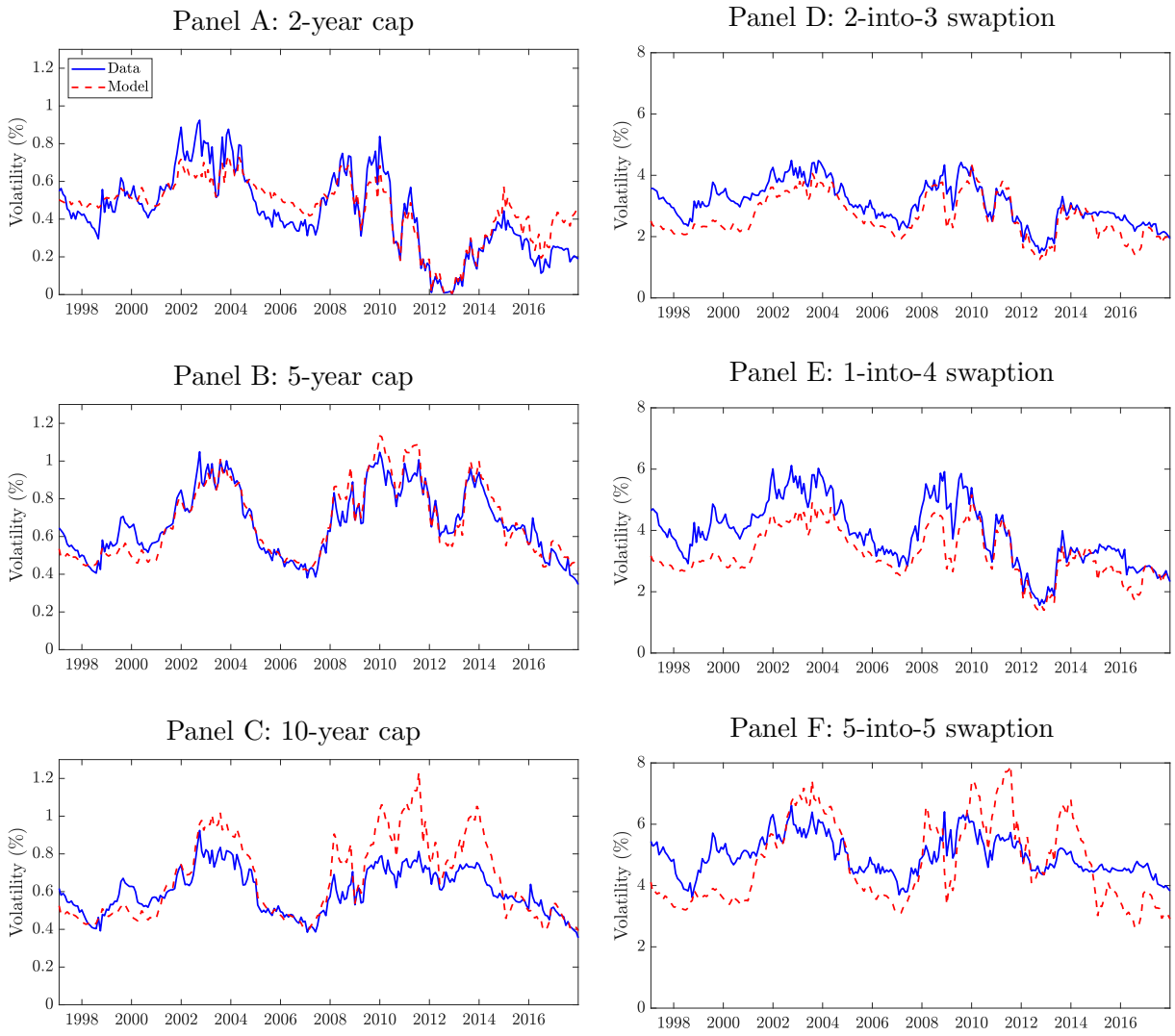

Notes: This figure plots the time series of the equivalent bond price volatilities for the 2-, 5-, and 10-year caps (Panels A, B, and C), and those for the 2-into-3, 1-into-4, and 5-into-5 swaptions (Panels D, E, and F) in the data and in the model, from January 1997 to December 2017. The solid blue lines represent the data, and the dashed red lines represent the model. All values are expressed in percentage terms.

Figure 7: Implied Time-Varying Disaster Risk

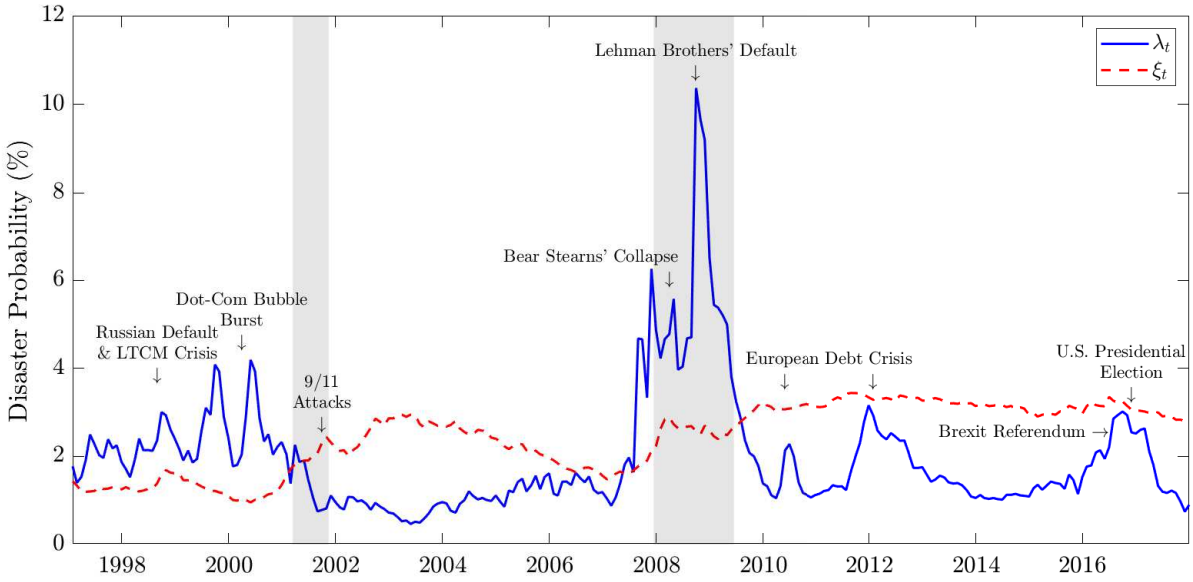

Notes: This figure displays the filtered time series of the short-run disaster risk component λ_t (solid blue line) and the long-run disaster risk component ξ_t (dashed red line), from January 1997 to December 2017. All values are expressed in percentage terms.

Figure 8: Disaster Risk, TED Spreads, and Interbank Rate Option-Implied Volatilities

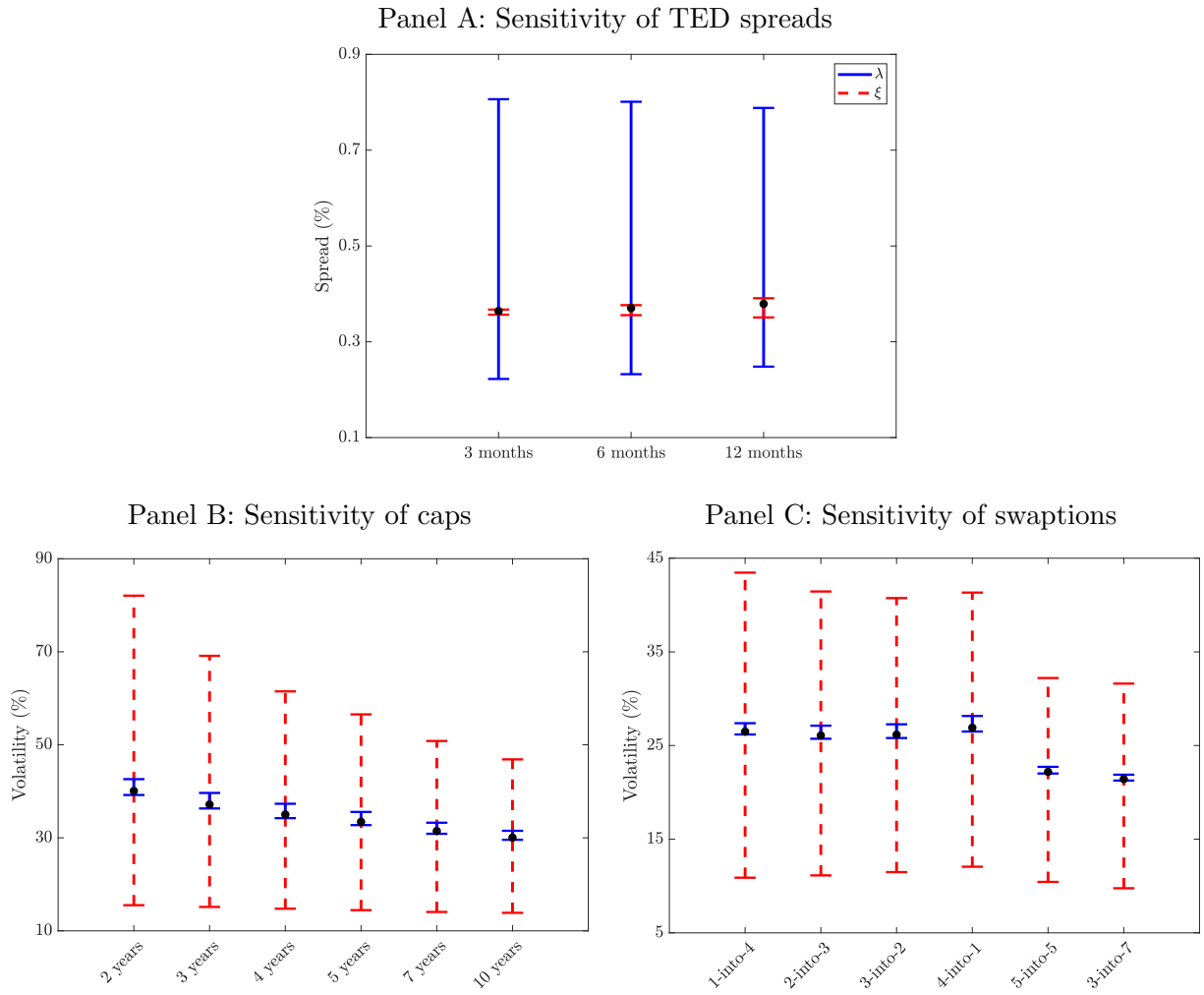

Notes: This figure shows how TED spreads (Panel A) and Black-implied volatilities for caps (Panel B) and swaptions (Panel C) change when λ_t or ξ_t varies from the 10th percentile to the 90th percentile of its filtered values. In each panel, the solid blue lines describe the sensitivity with respect to λ_t while fixing ξ_t at the median, whereas the dashed red lines describe the sensitivity with respect to ξ_t while fixing λ_t at the median. Expected inflation q_t is set at its median value in both cases. The black dot in the middle of each bar graph represents a model value when λ_t and ξ_t are both at their median values. All values are expressed in percentage terms.